Studies of Markers of Vasculature and Immunological Systems in Eyes of Lumpfish, a

North Atlantic Teleost

By ©Tatiana Hyde

A Thesis Submitted to the School of Graduate Studies in partial fulfilment of the requirements

for the degree of

Masters of Science in Medicine (Cancer and Development)

Division of Biomedical Sciences, Faculty of Medicine

Memorial University of Newfoundland

October 2022

St. John's Newfoundland and Labrador

Abstract

Lumpfish (*Cyclopterus lumpus*), a North Atlantic teleost, is used as a cleaner fish to delouse salmon in the commercial Atlantic Salmon (*Salmo salar*) farming industry. Lumpfish require high visual acuity to observe and consume prey, such as the louse on salmon skin. Hematopoiesis, a process in which stem and progenitor cells differentiate to form blood cellular components occurs primarily in the bone marrow, but during fetal development it can in rare cases occur in "extramedullary" structures such as the ocular choroid vasculature of the eye. The choroid vasculature is a specialized vasculature that services the posterior retina and accounts for the majority of the blood flow to the eye. The comparable vasculature structures between lumpfish and human provide a new opportunity for a new model system for studying vasculature biology. I propose that the development of the posterior vasculature and hematopoiesis system of the lumpfish eye involves unique expression markers that exaggerate and support natural extramedullary hematopoiesis in ocular vascular structures. To date, there has been no report of such processes in the lumpfish eye. Here, I examined in lumpfish eyes, the expression of zonula occuldens-1 (ZO-1), chloride intracellular channel protein 2 (CLIC2), proliferating cell nuclear antigen (PCNA), cluster of differentiation 45 (CD45) and cluster of differentiation 10 (CD10), known markers of vascular and hematopoietic tissues in mammals. I studied the association of the aforementioned markers throughout the development of posterior ocular vascular and hematopoietic tissues of lumpfish. I found that CD45, CD10, CLIC2, PCNA and ZO-1 are not only present in the lumpfish eye throughout development, but also that CD10, CD45, CLIC2 and ZO-1 seem to be developmentally regulated. Characterizing the development of known markers of posterior ocular vascular-hematopoiesis-like tissues of lumpfish is important to gain a better

understanding of ocular tissue development, homeostasis, and response to stress as well as

provide new basic knowledge on these markers.

Lay Summary

Lumpfish, a North Atlantic marine fish, gets its name from a characteristic large cartilage lump on the back of a short, thick body. Lumpfish have been a target of the fishing industry for their roe as a caviar substitute but are now becoming useful tools in the salmon fish farming industry. Lumpfish are used as a cleaner fish as they eat parasitic lice off farmed salmon. To effectively see and remove the small louse from the salmon skin, lumpfish require excellent vision. The process in which blood components are created is called hematopoiesis. This process normally occurs in the bone marrow but during development it has been seen to occur in other places, such as the eye. Lumpfish eyes have many unique eye structures with similarities to human eyes that make them an ideal model for studying eye biology. To examine if the development of eye vasculature involves various expression markers that support hematopoiesis within the eye, I examined four known markers of vascular and hematopoietic tissues over a developmental time course. The results of this study will allow for a better understanding of eye development and the function of each marker of interest.

Co-authorship Statement

      All individuals listed below have influenced the work of this thesis manuscript and have obtained authorship. Tatiana Hyde was primarily responsible for this thesis. Tatiana Hyde performed all immunohistochemistry experiments, captured histological images, collected, and analyzed all data. Tatiana Hyde completed the histological sectioning of all the larvae specimens, juvenile specimens LF375/376 and LF380, adult specimens LF402, LF 403 and slides 1-85 of LF 401. Preparation of the thesis was completed by Tatiana Hyde. Dr. Robert Gendron and Dr. Hélène Paradis acted as co-supervisors of the project, and both contributed to the study design as well as participated in the preparation, revision, and final acceptance of the thesis, and also undertook specimen collections, harvesting and processing. Dr. Robert Gendron provided guidance on how to conduct immunohistochemistry experiments and stain development as well as assisted in capturing some histological images. Dr. Robert Gendron and Dr. Hélène Paradis assisted in choosing the best representative immunohistochemistry images for each figure. Dr. Hélène Paradis participated in the western blot work and oversaw data analysis. Dr. Hélène Paradis conducted the CD10 and CD45 western blot depicted in Figure 2A and created Figure 2A. Dr. Giuseppe Scapigliati provided the CD45 DLT22 antibody as a kind gift. The CD45 DLT22 antibody was developed by Dr. Giuseppe Scapigliati and his team from the University of Tuscia in Viterbo, Italy. Iliana Dimitrova, medical laboratory technologist and histology unit supervisor at Memorial University of Newfoundland provided instruction and teaching on how to conduct histological sectioning. Iliana Dimitrova and Danielle Gardiner, medical technologists within the histology laboratory of Memorial University of Newfoundland conducted all paraffin embedding procedures and completed histological sectioning slides 86-187 of specimen LF401

for this project. The department of Ocean Sciences embedded and sectioned juvenile specimens

LF373 and LF 380.

Acknowledgements

Table of Contents

List of Tables

List of Figures

List of Abbreviations

AP	Alkaline Phosphatase
BSA	Bovine Serum Albumin
BLAST	Basic local alignment search tool
CD10	Cluster of differentiation 10
CD45	Cluster of differentiation 45
CE	Corneal Epithelium
CLIC	Chloride Intracellular Channel
CLIC2	Chloride Intracellular Channel 2
C. lumpus	Cyclopterus Lumpus
CMZ	Ciliary Marginal Zone
Dph	Days Post Hatch
ECL Block	Enhanced Chemiluminescence Advanced Block
H&E	Hematoxylin and Eosin
HK	Head Kidney
HRP	Horse Radish Peroxidase
IACC	Institutional Animal Care Committee
IHC	Immunohistochemistry
JBARB	Dr. Joe Brown Aquatic Research Building
mAB	Monoclonal Antibody
OSC	Ocean Science Center
PBS	Phosphate Buffered Saline
PCNA	Proliferating Cell Nuclear Antigen

PFA	Paraformaldehyde
RBC	Red Blood Cell
RLM	Retractor Lentis Muscle
RM	Rete Mirabile
RPE	Retinal Pigment Epithelium
SDS-PAGE	Sodium Dodecyl Sulfate Polyacrylamide Gel
t	Tapetum
TBS	Tris Buffered Saline
TBST	Tris Buffered Saline + Tween 20 25%
um	micrometer
ZO-1	Zona Occludens-1

Chapter 1: Introduction

1.1 Lumpfish

Teleosts are a large group of fish that can be found in both marine and freshwater habitats (Kolosov et al., 2013). *Cyclopterus lumpus*, commonly known as lumpfish are a predatory marine teleost of the class Actinopterygii and family *Cyclopteridae*. Lumpfish possess a short, thick body that does not possess any scales. Instead, they have numerous rows of tubercle protrusions along the body as well as a large cartilaginous dorsal hump in place of a dorsal fin that increases in size with age (Davenport, 1985). This teleost possesses a distinctive circular adhesive disc located on the ventral underbelly which is thought to have evolved from the pectoral fins. Lumpfish are relatively poor swimmers as they lack a swim bladder and use this adhesive disc to secure themselves to ocean rock, seaweed or when grown in culture, used to adhere themselves to holding tanks (Powell et al., 2018; Fisheries and Oceans Canada. 1996). Mature lumpfish range in size, usually between 40 to 60 cm in length. Females are typically larger than males in both length and weight (Fisheries and Oceans Canada. 1996). During early development, young lumpfish vary in colour to adapt to their surroundings. Adult lumpfish range from a blue-green to a pale grey-brown. However, during spawning season males appear bright red in colour (Fisheries and Oceans Canada. 1996). Lumpfish diet can differ depending on their relative size (Ingólfsson & Kristjánsson, 2002). Juveniles feed largely on copepods while the adult lumpfish diet consists of larger crustaceans, jellyfish, worms and some other smaller fishes such as herring and sand lance, thus they require high visual acuity to observe and consume prey (Ahmad et al., 2019; Eriksen et al., 2014).

Lumpfish can be found in a wide range of marine habitats along both sides of the

Atlantic from the coasts of Hudson's Bay, Maine, and Newfoundland to as far east on the

Atlantic as Norway (Mortensen et al., 2020; Fisheries and Oceans Canada. 1996). Large

concentrations of lumpfish can be found off the coast of Newfoundland (Fisheries and

Oceans Canada. 1996). Lumpfish were once thought to be a primarily benthic species but

are now known to live semi-pelagically as they inhabit both the pelagic and demersal

zone (Kennedy et al., 2015; Mortensen et al., 2020). During spawning season, which

occurs during the spring and summer months, lumpfish exhibit homing behaviour in

which they return to the same areas to breed. In addition to homing behaviour, lumpfish

follow specific courtship procedures as well, which include nest cleaning, fin brushing

and body quivering (Goulet et al., 1986). Lumpfish migrate to shallow, rocky water to

breed, seeking shelter in rocks and seaweed (Powell et al., 2018; Davenport, 1985). The

egg nests are estimated to contain between 150,000 to 280,000 eggs (Benfey & Methven,

1986). After the eggs have been fertilized by the males, female lumpfish leave the

breeding site to return to deeper waters while the male lumpfish remain at the nesting site

to guard and protect the fertilized eggs for 6-10 weeks (Davenport, 1985). The male

lumpfish fan and puff the egg masses to aerate the mass, when the larvae hatch, the larvae

are swept away from the nest site by these behaviours and dispersed into the water

(Goulet et al., 1986).

Prior to the 20th century, lumpfish had very little economic value and when caught as

bycatch were used as bait fish or animal feed (Powell et al., 2018). Lumpfish roe was

seen as a substitute for sturgeon caviar in the late 20th century making them a target for

the fishing industry (Powell et al., 2018). More recently, lumpfish have been found to be

useful tools in the fish farming industry. Sea lice (*Lepeophtheirus salmonis*) are one of the largest threats to salmon aquaculture as the lice have become resistant to many anti-parasitic therapies. Due to such chemotherapeutic resistance as well as the high costs of pharmacological therapies, the use of lumpfish as cleaner fish has become increasingly popular within the salmon aquaculture industry (Garcia de Leaniz et al., 2022; Powell et al., 2018). The lumpfish locate the sea lice on the salmon skin and remove and eat it. The use of lumpfish as a cleaner fish has become increasingly more apparent as they can withstand cold water temperatures, are more cost effective and less stressful to the farmed fish than medications or therapeutics (Powell et al., 2018).

According to the Committee on the status of Endangered Wildlife in Canada (COSEWIC), the status of lumpfish is threatened, while the International Union for Conversation of Nature (IUCN) classifies them as a near threatened species (Lorance et al., 2015; Committee on the Status of Endangered Wildlife in Canada [COSEWIC], Government of Canada). The exact cause of the decline in the lumpfish species is unknown but suspected to be caused by invasive species that may feed on lumpfish eggs, disease-causing infection, and climate change (Gendron et al., 2020; Powell et al. 2018; Committee on the Status of Endangered Wildlife in Canada [COSEWIC], Government of Canada). More research on lumpfish is required to not only better understand the use of lumpfish as a biological control agent but for their overall species survival as well.

1.2 Lumpfish as a Model System

Teleost fish are a beneficial scientific model, particularly for studying developmental biology as they produce large numbers of spawn, have external

fertilization and relatively quick development. Moreover, teleosts continue to grow throughout life and many tissues have the ability to regenerate, these factors generally result from the continual generation of new cells by tissue specific stem cells (Hitchcock & Raymond, 2004).

Lumpfish, a predatory marine teleost, are a relatively new model system of scientific study. Within the past decade they have been found to be excellent biological control agents in the aquaculture industry (Garcia de Leaniz et al., 2022; Gendron et al., 2020; Powell et al., 2018). Due to their importance in aquaculture, lumpfish are a teleost of both scientific and economic value to study. To date, knowledge about lumpfish development, their immunological systems and the species generally is limited. This makes them a novel model system to study and to date, the Gendron/ Paradis Laboratory group is the only group to have studied lumpfish eye development. Previously, a drawback to the use of lumpfish as a model system was that because they were severely under studied, their reference genome was unavailable. However, as of November 2019, the lumpfish genome has been mapped, published, and readily available to researchers (RefSeq assembly accession GCF_009769545.1). Development and the genes required for development in mammals are conserved within teleosts (Witten et al., 2017). Furthermore, as lumpfish are visually guided predators, an overall understanding of their ocular system and eye development is important in their implementation in aquaculture.

Lumpfish are an excellent model system because they are readily available in aquaculture allowing them to be easily acquired for scientific purposes. When lumpfish spawn they produce very large egg masses that contain hundreds of thousands of eggs (Benfey & Methven, 1986). Lumpfish also externally fertilize the eggs, which allows for

artificial fertilization to be conducted in captivity to result in more uniform embryo

development with increased chance of survival (Powell et al., 2018). Along with the

ability to be cultured, wild lumpfish can be domesticated and used for scientific research.

As with many other teleosts, such as the popular zebrafish (*Danio rerio*), lumpfish are an

excellent model system for studying developmental biology. The overall size of the

lumpfish eye is much larger than that of the eye of a zebrafish. This difference is

beneficial as the larger features are easily distinguishable in both histological and gross

dissection of the eye. Lumpfish continue to grow throughout development, including

organs such as their eyes. Lumpfish eyes harbor some features in common with mammals

but also other unique characteristics which might confer special capabilities in this

species. Lumpfish have exaggerated ocular anatomical and physiological structures of

blood vessels in the eye which allows one to ask questions at an expression level and

compare to humans. The continual growth of the eye, exaggerated vascular structures,

and the relative similarities to humans make them an excellent model system to study

ocular developmental biology. Lumpfish eyes harbor a robust choroid body, a structure

similar to choroid vasculature in mammals, as well as an extensive rete mirabile (Ahmad

et al., 2019). Characterizing the expression of various immunological (CD10, CD45) and

tight junction (CLIC2, ZO-1) related proteins and how they are potentially differentially

regulated throughout development is important as it may help to better understand the

role of immunological systems in ocular homeostasis in order to better protect lumpfish

from potential infectious disease.

1.3 Lumpfish Development

The literature on the characterization of lumpfish development through adulthood is limited. Information on lumpfish length-weight relationship is present for early post hatch fish and provides evidence that growth during the larval stages is rapid but there is little data present within scientific literature for lumpfish development past 45 mm in length, corresponding to the early juvenile stage (Powell et al., 2018). Further information on lumpfish development is required. Lumpfish eggs hatch 6-10 weeks post fertilization depending on various factors, such as water temperature (Imsland et al., 2019). Lumpfish post hatch development can be broken down into three stages: larval, juvenile and adulthood. The larval stage is classified as 1-50 days post hatch (dph). At the start of this stage the hatched larvae are 4-5mm in length. Day 0 to the end of the larval stage is a period of significant development as the lumpfish body is undergoing many changes and significant growth (Brown, 1986; Fisheries and Oceans Canada, 1996). The juvenile stage is classified as 50-250 dph and juvenile lumpfish can range between 5-7.5 cm in length (Brown, 1986; Fisheries and Oceans Canada, 1996). For almost the entire first year of life, juvenile lumpfish remain in shallow water, after which they migrate to increased depths (Brown, 1986; Fisheries and Oceans Canada, 1996). Adulthood is classified as greater than 250 days post hatch. During adulthood females can grow upwards of 61 cm while males range from 35.6-38.1 cm. The age of sexual maturation for lumpfish is thought to be about 2-3 years of age (Brown et al., 1992).

1.4 The Eye

The eye is a complex organ that converts light that passes through the cornea into electrical impulses that are sent to the brain to convert them into a representation of the external world. The eye is composed of many layers (Figure 1). The most exterior layers of the eye include the anterior cornea and the posterior sclera. The cornea functions to refract and transmit light to the lens while also serving to protect the eye from damage or infection (Willoughby et al., 2010). The cornea is densely innervated by sensory nerves. It is an avascular structure that is composed of five layers including, the epithelium, Bowman's membrane, the stroma, Descemet's membrane and endothelium. The corneal epithelium is largely impermeable because of the presence of cell junctions (Willoughby et al., 2010). The sclera is the outer layer of strong connective tissue that functions to maintain the eye shape and protect the eye from damage. The sclera and cornea are connected at the limbus (Figure 1). Posterior to the cornea but anterior to the limbus is the anterior chamber. The aqueous humour which is found within the anterior chamber is a clear fluid that provides the lens and cornea with nutrition, stabilizes the ocular structure, and aids in the regulation of ocular homeostasis (Goel, 2010).

The iris not only provides the colour of the eye but also functions to control the amount of light that enters the eye by either dilating or constricting the pupil, found in the center of the iris, to adjust its size and amount of light entering. Under low light conditions the iris constricts resulting in dilation of the pupil to increase the amount of light entering eye. However, if the external light is bright, the iris relaxes to constrict the size of the pupil which allows for less light to enter the eye. Posterior to the iris is the lens. The lens is a transparent, crystalline structure that functions to transmit light and

focus it on the retina. It consists of the lens capsule, epithelium, and lens fibres and the lens is suspended and held in place by the ciliary body (Figure 1) through zonule ligaments (Ruan et al., 2020). Lens accommodation allows for objects at a distance to be seen clearly. It is initiated by the contraction of the ciliary muscle to change the shape of the lens. When looking at objects at a distance, the ciliary body relaxes, increasing the tension on the lens zonules making the lens more flat. While when observing closer objects, tension on the zonules is reduced because the ciliary body contracts and this increases the convexity of the lens (Ruan et al., 2020).

From the lens, the light that has entered the eye passes through the vitreous humor (Figure 1) and projects to the retina. The vitreous humour is a transparent, gel like substance that functions to provide nutrients to the lens and support the transmission of light to the retina (Murthy et al., 2014). The retina (Figure 1) is comprised of various layers and cellular components. When light reaches the retina, it passes through the retinal layers and activates the photoreceptors. The photoreceptors convert the light into electrical signals, which travel via the optic nerve to the brain. The brain then creates the image we see. The choroid vasculature (Figure 1) and retinal vessels supply the retina with blood and nutrients. The choroid mainly consists of blood vessels and supplies the outer retina while also playing a role in thermoregulation (Nickla & Wallman, 2010).
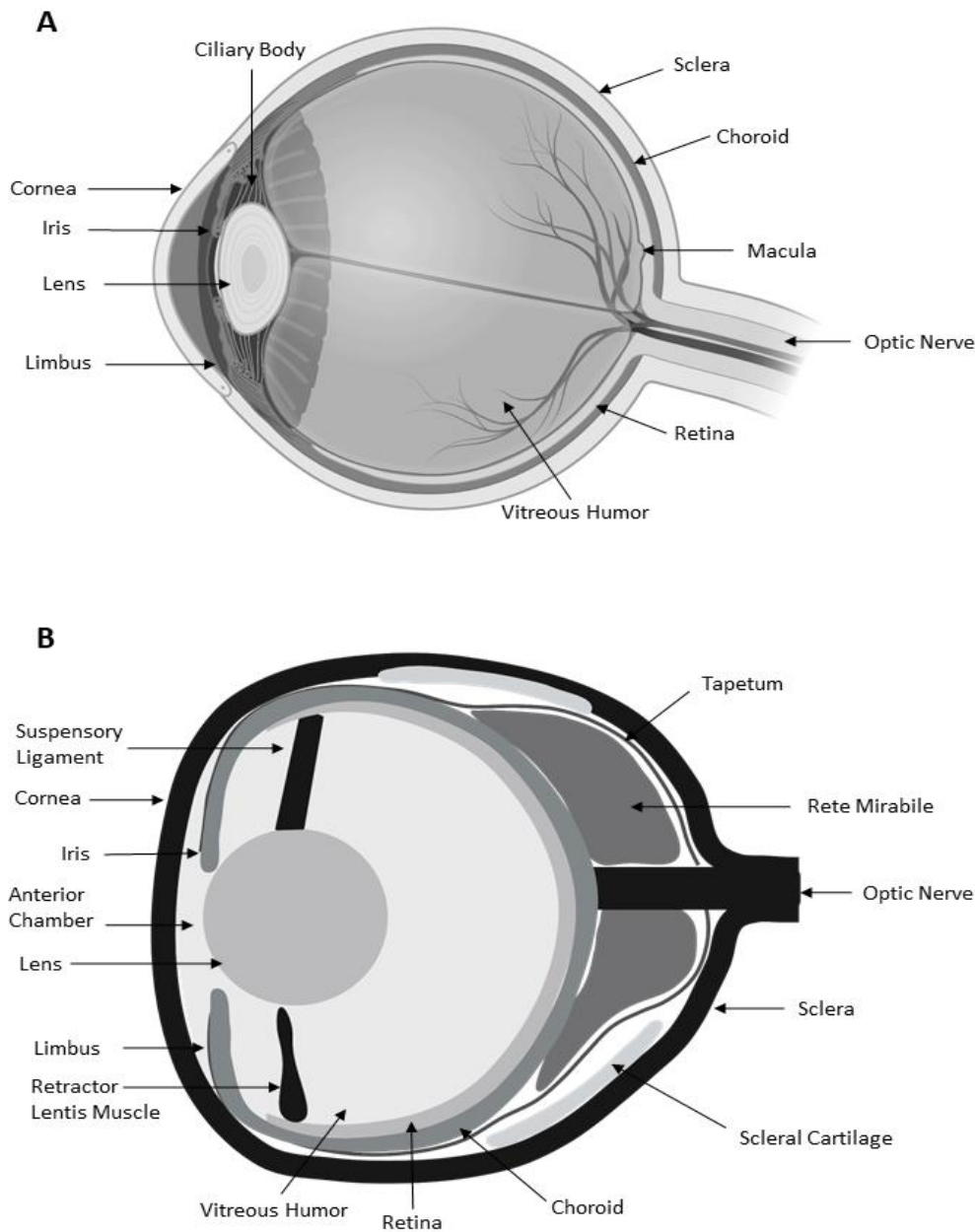
Figure 1. Anatomy of the (A) human eye versus the (B) lumpfish eye. A, From anterior to posterior, human eye structures include the cornea, limbus, iris, lens, ciliary body, vitreous humor, macula, retina, choroid, sclera and optic nerve. **B**, From anterior to posterior, lumpfish eye structures include the cornea, limbus, iris, lens, suspensory ligament, retractor lentis muscle, vitreous humor, retina, tapetum, choroid, sclera, scleral cartilage, optic nerve and rete mirabile. Many human eye structures are conserved in lumpfish. However, they possess unique structures such as the suspensory ligament and retractor lentis muscle to hold lens in place as well as a unique rete mirabile. Figure A is a generated image from *BioRender.com*. Figure B is an original image generated using *BioRender.com*.

1.5 Teleost vs. Mammalian Eye

Teleosts are known to be excellent models for studying human ocular development (Kitambi et al., 2011). Lumpfish eyes specifically demonstrate a high similarity to mammalian eyes. Many mammalian eye structures are conserved within the lumpfish eye (Figure 1) including the cornea, sclera, iris, limbus, lens, retina (including the same retinal layers as the mammalian eye), as well as the optic nerve. Such anatomical similarities to the mammalian eye, the continual growth of the eye within the lumpfish model, as well as the lumpfish eye being larger in size than that of the zebrafish, allow lumpfish to be an excellent model system to study ocular development. However, the lumpfish eye also possess some unique anatomical features such as the suspensory ligament, the retractor lentis muscle, the tapetum, and a rete mirabile.

In humans, the cornea is the main refractive element of the eye (Andison & Sivak, 1994). However, in teleosts, the cornea is optically inactive as the refractive index of the cornea is very similar to the index of water (Andison & Sivak, 1994; Khorramshahi et al., 2008; Kunz, 2004). Thus, the lens is the structure responsible for refracting and focusing light (Andison & Sivak, 1994; Khorramshahi et al., 2008; Kunz, 2004). The spherical crystalline teleost lens is very heavy and can not be held in place by the iris. The lens is firmly held and suspended in place within the eye by a dorsal suspensory ligament and a ventral retractor lentis muscle (Khorramshahi et al., 2008). In mammals, the ciliary muscle focuses the lens by contracting or relaxing to change the shape of the lens. This process in mammals is termed lens accommodation (Ruan et al., 2020). Lens accommodation does not occur in teleosts, instead lens displacement occurs by moving the lens backward towards the retina in response to the contraction of the retractor lentis

muscle (Kunz, 2004). The retractor lentis, a structure which contains smooth muscle, originates from the anterior end of the falciform process and inserts into the lens capsule through a transparent ligament (Andison & Sivak, 1994).

The tapetum lucidum present in the lumpfish eye is composed of cell supported crystallized guanine that functions to reflect light back into the eye and is considered to be one of the specialized structures for increasing photosensitivity in environments with poor light (Somiya, 1980). There are two types of tapetum lucidum in teleosts, one which is found in the choroid and another which is found in the retinal pigment epithelium of the retina (Ollivier et al., 2004; Somiya, 1980).

The ciliary marginal zone, found in teleosts, amphibians, birds and mammals, which is located in the periphery of the neural retina contains retinal stem and progenitor cells (Angileri & Gross, 2020; Fischer et al., 2013; Reh & Fischer, 2001). However, these cells only continue to proliferate in fish. In fish, the most central portion of the retina is generated during embryogenesis and the retina continues to grow throughout life by the generation and addition of new retinal neurons from the ciliary marginal zone (Fischer et al., 2013; Reh & Fischer, 2001). The ciliary marginal zone also contributes to the regeneration of damaged retinas in frogs and fish by replacing the damaged cells (Fischer et al., 2013; Reh & Fischer, 2001). It is not fully known if an analogous structure exists in mammals although there are active progenitor-like cells in the peripheral retina of mammals during embryogenesis (Angileri & Gross, 2020).

Lastly, the rete mirabile is an unique structure within teleost fish (Ahmad et al., 2019). The rete mirabile, also termed the choroid body, originates from a branch of the ophthalmic artery (Wittenberg & Wittenberg, 1974) and is a large, horseshoe shaped

body of blood vessels that extends around the optic nerve and rests on the choriocapillaris (Kunz, 2004; Wittenberg & Wittenberg, 1974). The rete mirabile not only supplies the teleost retina with blood and nutrients but also acts as a counter current exchanger to largely supply oxygen to the retina at a low partial pressure (Ubels et al., 1984; Wittenberg & Wittenberg, 1974).

1.6 Vertebrate Eye Development

Eye development is generally conserved among vertebrates. Following gastrulation, the eye field is specified with the formation of the optic sulci which are bilateral indentations in the prospective forebrain (Heavner & Pevny, 2012; Kitambi et al., 2011). Both eyes develop from a singular eye field that is divided into the bilateral hemispheres. Sonic hedgehog (*shh*) is expressed in the ventral forebrain and prechordal mesoderm, and is critical for the eye field to differentiate into the bilateral hemispheres (Heavner & Pevny, 2012). The vertebrate eye then arises as an invagination of the diencephalon forms the optic vesicles (Heavner & Pevny, 2012; Kunz, 2004). The optic vesicles then further invaginate to contact the surface ectoderm and form the lens placode (Heavner & Pevny, 2012). Before the optic cup is formed, retinal stem cells of the optic vesicle go through a series of patterning events to form regions that give rise to the retinal pigment epithelium, neural retina, and the optic stalk (Heavner & Pevny, 2012; Shaham et al., 2012). Once the optic vesicle is formed, the optic vesicle and lens placode invaginate to form the lens pit and optic cup. The lens pit then detaches from the ectoderm to become the lens vesicle (Shaham et al., 2012). The optic cup is bilayer, and the inner region of the optic cup becomes the presumptive neural retina while the outer layer becomes the presumptive retinal pigment epithelium (Heavner & Pevny, 2012; Kitambi et al., 2011).

Where the presumptive neural retina and retinal pigment epithelium meet gives rise to the iris and ciliary margin and this is a place of progenitor cells. Additional invagination of the optic vesicle occurs where the optic stalk encounters the ventral retina, and this produces the choroidal or optic fissure. This fissure provides space for blood supply and retinal axons (Heavner & Pevny, 2012). In zebrafish, it is known that endothelial cells enter the choroid fissure and form the retinal intraocular vasculature (Kitambi et al., 2011). However, nothing is currently known about blood vessel formation in the developing lumpfish eye. The optic cup then continues to grow until it closes over the choroidal fissure. Lens formation occurs as the lens stalk keeps the lens vesicle attached to the surface ectoderm. Upon detachment, the surface ectoderm then gives rise to the corneal epithelium (Heavner & Pevny, 2012; Kitambi et al., 2011). The anterior chamber then becomes fluid filled and mesenchymal cells move into the space between what will be the cornea and the outer edge of the optic cup forming the stroma of the iris and the ciliary body in mammals. The optic stalk continues to elongate and becomes the optic nerve (Heavner & Pevny, 2012).

Along with *shh*, there are various other genes and transcription factors required for proper eye development, most of which are conserved throughout vertebrates including *Pax6*, *Six3*, *RAX, Sox2, PAX2,* and *FGF* (Heavner & Pevny, 2012). *Shh* is required to induce the division of the eye field, failure for the eye field to divide into the two hemispheres results in cyclopia (Heavner & Pevny, 2012; Shaham et al., 2012). *Six3* is required for expression of *shh* in the diencephalon and is required for the formation of the eye and anterior forebrain through the inhibition of the Wnt signaling pathway (Shaham et al., 2012). *Six3* activates Shh in the ventral midline of the diencephalon (Graw, 2010).

Thus, loss of function mutations in *shh* and *Six3* in humans have been reported to lead to cyclopia as a result of midline defects (Heavner & Pevny, 2012). *Sox2* is a neural ectoderm transcription factor that activates *Rax* expression which is required for the upregulation of eye field transcription factors *Pax6* and *Six3*. Mutations in *Sox2* have been seen to result in either very small or a missing eye (Heavner & Pevny, 2012). Transcriptional regulators *Pax6*, *Six3* and *Sox2* and growth factor *Fgf* are particularly important for proper lens specification and development (Graw, 2010; Heavner & Pevny, 2012).

1.7 Lumpfish Ocular and Immunological Structures

1.7.1 Rete Mirabile

The retina of some teleosts relies on the rete mirabile and choriocapillaris to receive blood and oxygen. The rete mirabile is horseshoe shaped and non-pigmented structure that is referred to as the choroid body. It is located posterior to the retina and wraps around the optic nerve of the teleost eye (Ubels et al., 1984; Wittenberg & Wittenberg, 1974). It is a dense network of vasculature, the vessels of which are a similar in size to capillaries and originate from a pseudobranch of the ophthalmic artery (Damsgaard et al., 2020; Wittenberg & Wittenberg, 1974). The arterial and venous vasculature of the rete mirabile run in a parallel pattern and the flows of afferent and efferent blood are countercurrent (Wittenberg & Haedrich, 1974). The vessels of the rete mirabile supply the choriocapillaris to provide the posterior retina with blood (Wittenberg & Wittenberg, 1974).

Along with supplying blood, oxygen and nutrients to the posterior retina, the rete mirabile functions as a countercurrent exchanger as it maintains high oxygen tensions (Ali, 1975; Damsgaard et al., 2020; Wittenberg & Wittenberg, 1974). High partial pressures of oxygen are required to overcome diffusion as oxygen is supplied to the retina from diffusion by the choriocapillaris (Ali, 1975; Ubels et al., 1984). The choroid rete mirabile, which allows the high PO_2 to be magnified and localized behind the retina. The evolutionary innovation of the choroid rete provided a high oxygen flux to the thick fish retina without obstructing the optical path (Damsgaard et al., 2020).

1.7.2   Retina

The retina lines the posterior eye and is composed of several well-defined cellular layers that are derived from the neuroectoderm (Gupta et al., 2015). The layers of the retina include: the retinal pigment epithelium, the photoreceptor layer of rods and cones, outer nuclear layer, outer plexiform layer, inner nuclear layer, inner plexiform layer and the ganglion cell layer. The ganglion cell layer is the innermost portion of the retina that is closest to the lens while the rods and cones are the outermost layer of the retina that reside just anterior to the retinal pigment epithelium (Kolb, 2012). The retinal pigment epithelium is a single layer of cuboidal cells that contains melanosomes providing the pigmented colour (Gupta et al., 2015). It functions to absorb light that is focused on the retina, provides the rods and cones with nutrients from the blood and forms part of the blood retina barrier (Strauss, 2005). Rods and cones are specialized for different aspects of vision. The rods are

specialized cells for low light vision, and they do not perceive colour or have spatial acuity. While the cones are specialized for higher light levels, have high spatial acuity and are responsible for colour vision (Purves et al., 2001). The outer nuclear layer is made up of the cell bodies of the rods and cones. The outer plexiform layer is the location of synaptic activity between cone pedicles and rod spherules with many bipolar and horizontal cell types (Kolb, 2007). At this layer, two important synapses occur: the visual signal is differentiated into two channels, one that detects objects that are lighter than the background and another for darker images, and the second synapse creating contrast of the visuals (Kolb, 2007). The inner nuclear layer is made up of horizontal, bipolar and amacrine neuronal cells as well as Müller glia cells (Kolb, 2007; Masri et al., 2021). The inner plexiform layer comprises the synapses between bipolar, amacrine and ganglion cells (Zhang et al., 2021). Lastly, the retinal layer closest to the lens, the ganglion cell layer, consists of retinal ganglion cells (Momen et al., 2020).

In order for light to reach and activate the rods and cones it must travel through all layers of the retina. The photoreceptors contain opsin which is a G-protein-coupled receptor that contains a chromophore called 11-*cis*-retinal. When activated by light, signal transduction occurs to hyperpolarize the photoreceptors (Tsin et al., 2018). The electrical signal travels through all the layers of the retina to reach the optic nerve which transmits the visual signal to the brain (Kolb, 2012; Tsin et al., 2018).

While the mammalian retina and lumpfish retina are very similar, a major difference is blood supply. The mammalian retina receives blood supply from the

central retinal artery and the choroidal blood vessels (Kolb, 2012). The choroidal

blood vessels of the mammalian eye provide blood supply to the posterior retina

while the inner retinal layers are supplied by the retinal artery and capillaries (Kolb,

2012). The blood supply of many teleost species, including the lumpfish, is obtained

from the rete mirabile and choriocapillaris. Another difference in the retinas of

mammals and teleosts lies in how the retina responds to light. Retinomotor

movements are normally found in animals with fixed pupils, as pupil dilation in

response to light is not present (Burnside et al., 1982). Retinomotor movements

function to reposition photoreceptor cells and pigment granules of the retinal pigment

epithelium in response to varying light conditions (Burnside et al., 1982). In teleosts

retinomotor movements are used to optimize the retina for varying light conditions

instead of the pupillary movements used by mammals (Burnside et al., 1993). In

bright light environments the rods of the retina elongate, while the cones contract, and

within the retinal pigment epithelium the melanin granules disperse (Burnside et al.,

1993). Such mechanisms allow for the cones to be positioned in such a way that they

receive incoming light first, whereas in dark environments the rods contract while the

cones elongate, and the melanin granules secure themselves into the cell bodies of the

retinal pigment epithelium. This allows for maximal exposure of light to the outer rod

cells (Burnside et al., 1993). It has also been found that this retinomotor mechanism is

not only affected by varying amounts of light but also through the natural circadian

rhythms (Burnside et al., 1993). This response has even been found in fish whose

habitat is constant darkness or there is a prolonged absence of bright light (Burnside

et al., 1993). Finally, teleost retinas also continue to grow throughout post-embryonic

development and have the capacity to regenerate (Otteson & Hitchcock, 2003; Sherpa et al., 2008). The continual growth of the teleost retina is a result of both hypertrophy, the increase in size of differentiated cells and hyperplasia which is the formation of new neurons (Otteson & Hitchcock, 2003). Whereas in mammals, neurogenesis is completed during pre- and peri-natal development, therefore injury to the retina of mammals results in irreversible damage (Otteson & Hitchcock, 2003; Sherpa et al., 2008).

1.7.3   Limbus

The limbus is the border zone between the cornea and the sclera and has an angular oval shape. The limbus functions to nourish the peripheral cornea, contains aqueous humour outflow and in humans, it is the site of incision for eye surgeries (Van Buskirk, 1989). The limbus is composed of limbal stem cells, limbal stromal fibroblasts, melanocytes, immune cells, macrophages, and vascular endothelial cells (Gonzalez et al., 2018). The limbal stem cells are a quiescent population of cells that can become highly proliferative to provide corneal regeneration and repair. In mammals, the limbus is one of the few stem cell niches that is conserved through adulthood (Gonzalez et al., 2018). The limbal stromal fibroblasts express various mesenchymal stem cell markers and *in vitro* can differentiate into adipocytes, osteocytes, vascular endothelial cells, and cornea-like epithelium (Gonzalez et al., 2018). The stromal cells can also suppress inflammation and restore transparency of damaged stromal tissue. The loss of limbal stem cells could result in inadequate wound healing and a disruption of corneal homeostasis. Loss of corneal homeostasis

could lead to loss of vision (Gonzalez et al., 2018). During eye field formation the surface ectoderm and neuroectoderm divide, resulting in the formation of the corneal epithelium. It is thought that the limbus is formed by the surface ectoderm and the periocular mesenchyme (Gonzalez et al., 2018).

1.7.4   Retractor Lentis Muscle

The lens of the teleost eye is a large and heavy crystalline structure that is not able to be held in place by the iris as it is in mammals (Khorramshahi et al., 2008; Soules & Link, 2005). The shape of the teleost lens is different than the mammalian lens. The mammalian lens is shaped as an ellipsoid whereas the zebrafish lens is shaped like a large sphere (Soules & Link, 2005). The lens of teleosts is securely held in place by the suspensory ligament and smooth muscle structure called the retractor lentis muscle (RLM) (Andison & Sivak, 1994; Khorramshahi et al., 2008). The RLM is smooth muscle which originates in the anterior end of the falciform process and inserts into the lens capsule through a transparent ligament (Andison & Sivak, 1994). Teleosts in turn, do not follow the same lens accommodation strategy as mammals (Ruan et al., 2020). Lens displacement occurs when the RLM contracts, moving the lens posteriorly towards the retina (Andison & Sivak, 1994; Khorramshahi et al., 2008; Kunz, 2004). Although teleosts do not possess a ciliary body like that of mammals, the similarities between teleost RLM and mammalian ciliary muscle include that they are both smooth muscle structures, are largely innervated by the parasympathetic nervous system and they lack gap junctions (Andison & Sivak, 1994; Somiya, 1987).

1.7.5 Cornea

The cornea is the transparent avascular tissue that makes up the outermost portion of the eye. The cornea is composed of five layers, from anterior to posterior these layers are: the epithelium, Bowman's layer, corneal stroma, Descemet's membrane and the endothelium (DelMonte & Kim, 2011). The corneal epithelium is made of non-keratinized, stratified squamous epithelium that is established from the surface ectoderm during eye development. The epithelial cells maintain tight junctional complexes to keep toxins and unwanted microbes from penetrating the deeper corneal layers (DelMonte & Kim, 2011). Bowman's layer is located posterior to the corneal epithelium and is composed of Type I and V collagen and functions to help maintain the shape of the cornea. The corneal stroma forms most of the cornea and is composed of keratocytes which are required to maintain the environment of the extracellular matrix. The transparency of the cornea is a result of the way in which the collagen fibers of the stroma are arranged. The stromal fibrils are made up of type I and V collagen fibers that are arranged in parallel layers throughout the stroma, although, when the fibrils approach the limbus, their arrangement is modified circumferentially (DelMonte & Kim, 2011). Lastly, the corneal endothelium is a single layer of cells that lines the posterior cornea (Van den Bogerd et al., 2019). The cornea relies on diffusion to receive nutrients from the aqueous humour. The corneal endothelium is a slightly permeable layer of cells that allows for a flux of ions from the corneal stroma to the aqueous humour (DelMonte & Kim, 2011; Van den Bogerd et al., 2019). The cornea of zebrafish possess a thicker epithelium while a thinner

stroma and endothelium in comparison to the mammalian cornea (Soules & Link, 2005).

The cornea functions to not only protect the eye structures but also focus light on the retina and, in mammals, the cornea largely contributes to the refractive power of the eye (DelMonte & Kim, 2011). However, the teleost cornea is optically inactive since, the water environment surrounding the teleost and the aqueous humour interior to the cornea inside the anterior chamber, have very similar refractive indices (Khorramshahi et al., 2008). Therefore, the lens is the area of refractive power for the teleost eye (Khorramshahi et al., 2008).

1.7.6 Tapetum

The tapetum lucidum is composed of cell supported hexagonal crystallized guanine that functions as a reflector system to reflect light in the retina (Ahmad et al., 2019; Ollivier et al., 2004; Somiya, 1980). By reflecting light in the retina, the tapetum provides the photoreceptors with another opportunity to become stimulated which in turn provides increased visual acuity at low light levels (Ollivier et al., 2004). There are two types of tapetum that have been examined in the eyes of fish: the choroid tapetum and the retinal tapetum. The choroidal tapetum is located just posterior to the choriocapillaris while the retinal tapetum is located adjacent to the retinal pigment epithelium (Ollivier et al., 2004). The tapetum is also thought to be at least partially responsible for the eyeshine phenomenon in animals, in which the eye itself seems very bright (Fritsch et al., 2017; Ollivier et al., 2004). The tapetum

(Figure 1), localized around lumpfish sclera, iris and retina have been found to vary in thickness and functions to reflect light within the retina (Ahmad et al., 2019).

1.7.7   Head Kidney

The kidney in teleost fish is located retroperitoneally on the dorsal wall of the body cavity (Press & Evensen, 1999). In teleosts, the head kidney is a soft tissue organ that is analogous to the adrenal gland in mammals and is the primary site of hematopoiesis. It is an important endocrine and hematopoietic-lymphoid organ comprised of immune, lymphoid and endocrine cells (Geven & Klaren, 2017). The head kidney is the site of all hematopoietic differentiation and along with being considered analogous to the mammalian adrenal gland, it is also said to be identical to mammalian bone marrow (Kobayashi et al., 2016). The head kidney also serves as a secondary lymphoid organ that is important in immune responses (Press & Evensen, 1999). There is a large network of sinusoids, supported by the stroma, within the parenchyma of the head kidney. The stroma is comprised of endothelial cells that line the sinusoids, adventitial cells and reticular cells (Press & Evensen, 1999). The stroma functions to support hematopoietic tissue of the head kidney but also has an immune function and clearance role. The macrophages and endothelial cells of the head kidney sinusoids trap debris from the blood and the renal portal system then filters and removes such debris (Press & Evensen, 1999). The head kidney also may play a role in teleost immunological memory as it is a major antibody producer. The accumulations of melanomacrophages within the head kidney parenchyma then retain

the antigens for extended periods of time following vaccination or infection (Press & Evensen, 1999).

1.8 Proteins Related to Tight-Junction and Immunological Response

1.8.1   CD10

CD10, also known as neutral endopeptidase, neprilysin or common acute lymphoblastic leukemia antigen, is a membrane-bound zinc-dependent endopeptidase (Maguer-Satta et al., 2011). CD10 was first identified as a tumor specific antigen in leukemia, and has since been found to be involved in mammalian stem cell regulation (Maguer-Satta et al., 2011). Within the immune system, CD10 is found to be present on the surface of neutrophils. It regulates neutrophil activation through the inactivation and degradation of inflammatory peptides. CD10 is a known marker for hematopoietic progenitor cells in mammals (Gendron et al., 2020; Maguer-Satta et al., 2011) and also plays a role in the maturation of B-cells (Maguer-Satta et al., 2011). CD10 metabolizes peptides by cleaving them between the hydrophobic residues, inactivating and reducing the concentration of functionally active peptides required for signaling. In addition to the enzymatic function of CD10, it is also involved in interfering with many major signaling pathways (Ding et al., 2020; Jana et al., 2014; Maguer-Satta et al., 2011). CD10 mediation can be controlled by both extracellular enzymatic activity and intracellular signaling pathways controlled by various hormones, cytokines or adhesion molecules such as phosphoinositide 3-kinase (PI3K) and p85, a subunit of PI3K, Lyn kinase, amongst others (Jana et al., 2014; Maguer-Satta et al., 2011). CD10 has been found to be involved with the

activation of focal adhesion kinase (FAK). CD10 coimmunoprecipitates with Lyn and p85 to block PI3K interaction with FAK, thus decreasing FAK phosphorylation and decreasing cell migration (Jana et al., 2014; Maguer-Satta et al., 2011). CD10 is also known to activate the protein kinase B (AKT) pathway through the phosphorylation of phosphatidylinositol (3,4,5)-trisphosphate (PIP3) following the association of CD10 and tumor suppressor phosphatase and tension homolog (PTEN). The AKT pathway can also be activated by CD10 through the cleavage of fibroblast growth factor 2, this inactivates endothelial cell growth and angiogenesis (Jana et al., 2014; Maguer-Satta et al., 2011).

1.8.2   CD45

Cluster of differentiation 45 (CD45), also known as leukocyte common antigen, is a receptor-linked tyrosine phosphatase expressed on all mammalian leukocytes (Altin & Sloan, 1997; Marozzi et al., 2012). It is expressed on all hematopoietic cells apart from erythrocytes and platelets (Marozzi et al., 2012; Rheinländer et al., 2018). There are various isoforms of CD45 obtained through alternative splicing, the isoform that is expressed is dependent on cell subpopulation, cell maturity and if the cells have been previously exposed to antigen (Altin & Sloan, 1997). However, the exact biological significance of CD45 isoforms is uncertain (Altin & Sloan, 1997; Marozzi et al., 2012; Rheinländer et al., 2018). CD45 expression is required for the activation of T cells. In T cells, CD45 activates lymphocyte-specific protein tyrosine kinase (Lck). It also dephosphorylates and downregulates Janus kinases (JAK) which activate the signal transducer and activator

of transcription pathway (STAT), which is a key regulator of cytokine expression (Marozzi et al., 2012; Rheinländer et al., 2018). Immunoregulatory processes involving CD45 correlate with barrier proteins allowing for CD45 to be used as an indirect measure of barrier. For example, in the retinal endo- and epithelium, CD45 is observed to present T cells with antigens following tissue destruction (Gregerson & Yang, 2003). In humans CD45 is seen to be present in many infections and diseases. CD45 plays a large role in the immune response and mutations in CD45 play a role in disease progression. It has been found to be associated with viral infection of HIV-1 (Rheinländer et al., 2018). When CD45 expression is reduced in virus-infected cell lines, apoptosis of infected HIV-1 cells is also reduced (Rheinländer et al., 2018). In oncological conditions such as childhood acute lymphoblastic leukemia and Hodgkin's lymphoma there is a loss of CD45 expression. Additionally, in various oncological conditions the level of expression of CD45 is crucial for a patient's prognosis (Rheinländer et al., 2018).

1.8.3   CLIC2

The family of chloride ion channel proteins (CLIC) has a single putative transmembrane domain and exists in membrane bound and cytosolic forms (Gururaja Rao et al., 2020; Zeng et al., 2018). CLICs have been established as multifunctional proteins and not just chloride channels, many different functions of CLICs have been determined making it difficult to define the specific nature and function of them (Gururaja Rao et al., 2020; Ueno et al., 2019). CLICs are thought to play a role in pH regulation, homeostasis, solute transport, and cell proliferation and differentiation

(Zeng et al., 2018). CLIC2, or chloride intracellular channel protein 2, is the least investigated protein of the six homolog CLIC family. CLIC2 is not found on the murine genome which makes it difficult to produce and observe a knockdown model, this is most likely the reason why CLIC2 is the most understudied protein of the CLIC family (Gururaja Rao et al., 2020; Ozaki et al., 2021; Ueno et al., 2019; Zeng et al., 2018). In humans, CLIC2 is found on the telomeric region of chromosome Xq28, the duplication or the lack of this gene has reportedly resulted in intellectual and developmental disabilities, atrial fibrillation, cardiomegaly and/or epilepsy mainly in male children (Gururaja Rao et al., 2020; Ueno et al., 2019). More recently, CLIC2 has been found to be highly expressed in non-cancerous blood vessel endothelial cells but is not present in cancerous tissues and was found to be co-expressed with other tight junction proteins (Gururaja Rao et al., 2020; Ozaki et al., 2021; Ueno et al., 2019). Thus, it is thought that CLIC2 might be involved in the formation and maintenance of endothelial tight junctions in non-cancerous tissues, which may aid in the prevention of cancer metastasis (Gururaja Rao et al., 2020; Ozaki et al., 2021; Ueno et al., 2019).

1.8.4   PCNA

Proliferating cell nuclear antigen (PCNA) was first identified in patients with systemic erythematosus as an autoantigen (Juríková et al., 2016; Kelman, 1997). Molecules of PCNA form a homotrimeric ring around DNA and acts as a sliding clamp that recruits and regulates protein binding (Wang, 2014). PCNA plays a vital role in the metabolism of nucleic acids, DNA replication, recombination and repair,

and cell cycle control (Juríková et al., 2016; Kelman, 1997). Due to its role in replication, it is a classic marker of cell proliferation (Ahmad et al., 2019; Juríková et al., 2016; Kelman, 1997). PCNA staining has been used as a marker of cell proliferation in hematopoietic tissues previously (Budke et al., 1994). In Zebrafish, PCNA has been seen to be exclusively expressed in hematopoietic tissues in the kidney (Leung et al., 2005).

1.8.5   ZO-1

Zonula occludens-1 (ZO-1) is a membrane associated tight junction protein that plays a vital role as a scaffolding protein to secure transmembrane tight junctions to the cytoskeleton (Georgiadis et al., 2010; Imafuku et al., 2021). ZO-1 consists of three PDZ domains, one guanylate kinase-like (GUK) domain and one Src homology 3 (SH3) domain making them a member of the membrane-associated guanylate kinase family (Umeda et al., 2006). It functions to link junctional membrane proteins and signalling plaque proteins to the cytoskeleton (Georgiadis et al., 2010; Imafuku et al., 2021). ZO-1 interacts with various junctional components of the endothelia including the claudin and junctional adhesion molecule (JAM) families (Tornavaca et al., 2015). ZO-1 may affect cell proliferation and gene expression in epithelial cells through the inhibition of ZO-1-associated nucleic-acid-binding protein (ZONAB), in a negative feedback loop (Georgiadis et al., 2010). The ZO-1/ZONAB pathway has been seen to regulate epithelial cell proliferation in culture as ZONAB interacts with cell cycle kinases to regulate the transcription of cell cycle genes such as PCNA (Georgiadis et al., 2010).

1.9 Rationale and Hypothesis

As highlighted above, the use of lumpfish as a model system is extremely novel and understudied. Lumpfish have become a useful tool in salmon farming as they are used as a biological control agent to remove sea lice from salmon skin (Powell et al., 2018). As a predatory teleost, lumpfish require high visual acuity to successfully pick lice on salmon skin as well as hunt and consume prey (Ahmad et al., 2019; Gendron et al., 2020). More research is required to further understand lumpfish development in general, as well as their ocular systems, specifically focusing on barrier and immune systems. Additionally, these findings are applicable to mammalian systems such as the human eye.

CD10 is a known stem cell and hematopoiesis progenitor marker (Maguer-Satta et al., 2011), CD45 is a receptor-linked tyrosine phosphatase that is expressed on leukocytic cells (Altin & Sloan, 1997) and ZO-1 is a known tight junction associated protein that links junctional membrane proteins to the cytoskeleton (Georgiadis et al., 2010). CD10 and CD45 are known hematopoietic and immune cell markers (Altin & Sloan, 1997; Gendron et al., 2020; Maguer-Satta et al., 2011) and work by Gerogiadis and colleagues (2010) found that ZO-1 may play a role in retinal pigment epithelium homeostasis in the eye. CLIC2, another marker of interest for this research is a novel marker as it is the least studied of the entire CLIC family (Ueno et al., 2019). Ueno and colleagues suggested that CLIC2 may act similarly to ZO-1 (Ueno et al., 2019). With this knowledge, it is hypothesized that the development of the posterior vasculature and hematopoiesis system of the lumpfish eye involves barrier and immune related expression markers that exaggerate and support ocular posterior vascular structures. The aim of the study is to characterize expression of known markers of vascular and hematopoietic tissues

associated with the development of the posterior ocular vascular versus hematopoietic tissue of lumpfish across a developmental time course. A better characterization of this development is needed to understand its role in ocular tissue development, homeostasis and stress responses. Conducting a developmental analysis not only provides the opportunity to test and determine if the proteins are developmentally regulated but could also provide new insights on the function of each protein as well as provide insight on approaches for exploring each proteins function.

1.10   Summary of Findings

Western blot analysis was conducted to confirm the location of expression for CD10, CD45, CLIC2 and ZO-1 that was indicated by the immunohistochemistry findings. Western blot analyses were performed on adult lumpfish retina and lumpfish rete mirabile tissues. Immunohistochemistry was performed on paraffin wax sections of whole-body lumpfish larvae, 20 and 48 dph, whole head of juvenile lumpfish 85, 118 and 150 dph and whole adult lumpfish eye, 263 and 606 dph to determine the expression of CD10, CD45, CLIC2, PCNA and ZO-1. I found that CD10, CD45, CLIC2, PCNA and ZO-1 were all expressed in various structures of the lumpfish eye. Interestingly our results suggest that CD10, CD45, CLIC2, PCNA and ZO-1 are not only present in the lumpfish eye throughout development but also that CD10, CD45, CLIC2 and ZO-1 seem to be developmentally regulated. Determining expression of these markers within lumpfish ocular tissue, as well as examining developmental regulation, is extremely novel. To our knowledge, Gendron/ Paradis group is the only group, to study lumpfish

29

ocular development. The findings of this work provide new knowledge about each

marker's expression.

Chapter 2: Materials and Methods

2.1 Fish Collection

Fish collection and processing was approved by the Institutional Animal Care Committee (IACC) of Memorial University of Newfoundland. *C. lumpus* were cultured and cared for at the Ocean Sciences Center of Memorial University, within the Dr. Joe Brown Aquatic Research Building (JBARB). Whole body larvae, whole head and eye tissues were collected from lumpfish specimens over a developmental time course from larval stage to adult. Ages of specimens collected include 20 days post hatch (dph), 48 dph, 85 dph, 118 dph, 263 dph and 606 dph.

Fish larvae at ages 20-48 dph were placed directly in 4% paraformaldehyde in phosphate buffered saline (PBS) and fixed for 48 hours as a means of rapid euthanasia without the destruction of eye tissue. Larger specimens were rapidly euthanatized by cervical dislocation using a scalpel to separate the body and head without causing damage to the ocular tissue. Following cervical dislocation, whole heads of early juvenile of 85 dph and 118 dph *C. lumpus* specimens were immersed and fixed in 4% paraformaldehyde in PBS (1.6 g paraformaldehyde, 40 ml PBS). The 85 dph specimen was fixed for 48 hours while the 118 dph specimen was fixed for 72 hours. For adult fish specimens the eyes were removed from the head following cervical dislocation before fixation in 4% paraformaldehyde. Adult eye 263 dph tissues were fixed for 24 hours while the sclera of the 606 dph specimen was pierced and the eye was fixed for 72 hours. After fixation, tissues were rinsed twice in PBS and placed in 70% ethanol for paraffin embedding.

Lumpfish tissues, including, lumpfish rete mirabile, retina, lumpfish head kidney and whole eye were removed, placed in RIPA2++ lysis buffer (Table 2.1) that was prepared as

31

previously described (Paradis et al., 2008) and frozen in liquid nitrogen. These tissue samples were frozen and stored at -80^0C for future protein extraction and Western blot analysis.

Reagent	Concentration
Tris	20 mM pH 7.6
Glycerol	10%
NaCl	137 mM
SDS	0.1%
Triton X 100	1%
EDTA	2mM
Na Deoxycholate	0.5%
Sodium Orthovanadate	1 mM
DTT	1 mM
Leupeptin	100 ug/ml
Aprotinin	10 ul/ml
NaF	50 mM
β - glycerophosphate	25 mM
Phenylmethyl-sulfoxide (PMSF)	1 mM
H_2O	

Table 2.1: RIPA 2++ Reagents

2.2 Paraffin Embedding and Tissue Sectioning

C. lumpus larvae, head and eye tissues were processed for paraffin embedding by the histology laboratory team at Memorial University of Newfoundland Faculty of Medicine. The tissue specimens were placed in histology cassette in a specified orientation, covered with paraffin and left to harden. Serial sections 5 um wide were cut through larvae, head and eye sections using a Leica RM2255 microtome. Some sections were cut by the histology department at the Ocean Sciences Centre, some by the histology department at within the Faculty of Medicine and others sectioned within the lab by Tatiana Hyde. The specimen block was initially iced for 45-60 minutes and sectioned at 5 um thick using a Leica RM2255 microtome. Two sections were deposited on Superfrost Plus slides (Thermo Fisher). Every twenty paraffin sections of each tissue specimen were stained with hematoxylin (50g Aluminum potassium sulphate, 1g Hematoxylin, 0.1g sodium iodate, 1g citric acid, 50g chloral hydrate, 1 L deionized dH$_2$O) and eosin (495 mL dH$_2$O, 2.5g Eosin, 5 mL Glacial Acetic Acid) staining while others were used for immunohistochemistry (IHC).

2.3 Bioinformatics

The protein sequences of each marker of CD45, CLIC2, PCNA and ZO-1, were acquired from the National Center for Biotechnology Information (NCBI) protein database: *Homo sapiens* ZO-1 (accession number AAA02981.1), *Homo sapiens* CLIC2 (NP_001280.3), *Dicentrarchus labrax* CD45 (CCD31440.1) and *Homo sapiens* PCNA (CAG38740.1). The FASTA sequence for *Homo sapiens* ZO-1, CLIC2 and PCNA as well as *Dicentrarchus labrax* CD45 was downloaded and inserted as the query sequence in Protein Basic Alignment Search Tool (BLAST) and *Cyclopterus lumpus* (taxid: 8103) was chosen as the search set.

33

2.4 Immunohistochemistry

Immunohistochemistry (IHC) was performed on paraffin wax sections of larvae, head, and eye tissue to determine the expression of CD45, CD10, CLIC2, PCNA and ZO-1. The sections were deparaffinized in xylenes for 15 minutes and then rehydrated using decreasing ethanol dilutions [100%, 95%, 70%, (2 mins) 50%, 30% (1 min)]. The tissues were then post fixed in 4% paraformaldehyde in PBS for 10 minutes and washed three times in tris buffered saline (TBS) (10mM tris pH 7.6, 150mM NaCl), each wash was 5 minutes. The sections then underwent antigen retrieval; for ZO-1 IHC the sections were incubated with trypsin (1mg/ml, 0.1%w/v in 150mM Tris pH 7.6, 3.3mM calcium chloride) for 11 minutes at 37^0C. For CLIC2, CD45 and CD10 IHC, the sections were incubated with 125 ul per slide of tris-ethylenediaminetetraacetic acid (EDTA) buffer (10 mM Tris base, 1 mM EDTA solution, 0.05% Tween 20, pH 9.0) for 5 minutes at 95^0C and CD10 sections for 10 minutes at 95^0C using the Eppendorf Mastercycler gradient machine for antigen retrieval. No antigen retrieval was required for PCNA IHC (Ahmad et al., 2019). Following antigen retrieval, the sections were washed in TBS three times, circumscribed with an Immedge pen (Vector Laboratories) and incubated at room temperature for 1 hour with 2% Enhanced Chemiluminescence Advanced Block (ECL) block (GE Healthcare UK Limited) in TBS (1g ECL block, 50 mL TBS). For the PCNA IHC, the sections were washed three time in TBS, circumscribed with the Immedge pen and incubated at room temperature for 1 hour with 2% ECL block in TBS-TritonX100 (0.1%). The tissues were then incubated in primary antibodies (Table 2.1) diluted in 2% ECL block solution overnight at room temperature. The following day the sections were washed three times in TBS and incubated at room temperature for 2 hours with the appropriate secondary antibody (Table 2.1) diluted in 2% ECL block. Following secondary antibody incubation, sections were washed three

times in TBS and developed using Vector Red AP substrate (Vector Laboratories). Colour

development was observed under a compound light microscope and the development reaction

was stopped using two washes in tap water. Slides were inverted and allowed to dry overnight.

The dry slides were then mounted with Permount (Fisher Scientific) and dried overnight.

Antigen	Host	Antibody	Clone	Primary or Secondary Ab	Isotype	Ab Dilution	Source and Product #
CD10	Rabbit	Monoclonal	SP67	Primary	IgG	1/50	ab227640, abcam
CD45	Seabass	Monoclonal	DLT22	Primary	IgG	50/50	Scapigliati group[†], University of Tuscia
CLIC2	Rabbit	Monoclonal	EPR6494	Primary	IgG	1/50	ab175230, abcam
PCNA	Rabbit	Polyclonal	FL-261	Primary	IgG	1/75	sc-7907, Santa Cruz Biotechnology
ZO-1	Mouse	Monoclonal	ZO1-1A12	Primary	IgG	1/50	WA316684, Invitrogen
Rabbit	Goat	-	-	Secondary (AP)	IgG	1/200	S373B, Promega
Mouse	Goat	-	-	Secondary (AP)	IgG	1/200	115-055-205, Jackson
Mouse	Goat	-	-	Secondary (AP)	IgG	1/200	S372B, Promega

Table 2.2: Primary and Secondary Antibodies used in Immunohistochemistry Experiments
†(Marozzi et al., 2012)

2.5 Hematoxylin and Eosin (H&E) Staining

Mayers Hematoxylin was prepared by dissolving 50g aluminum potassium sulphate,

1g Hematoxylin, 0.1g sodium iodate, 1g citric acid, 50g chloral hydrate in 1L of dH_2O. The

solution was then filtered through Whatman No. 1 filter paper. Eosin staining solution was

prepared by dissolving 2.5g Eosin (Fisher Scientific) in 495 ml of dH_2O, filtered through

Whatman No.1 filter paper and 5mL glacial acetic acid was added. Slides including paraffin embedded tissue sections were examined and every twenty slides of the tissue set was used for H&E staining. The slides were deparaffinized using Xylenes (Fisher Scientific) for 15 minutes. Following deparaffinization, the slides were gradually re-hydrated using decreasing concentrations of ethanol [100%, 95%, 70%, (2 mins) 50%, 30% (1 min)]. The slides were then post-fixed in 4% paraformaldehyde in PBS for 10 minutes. Slides were rinsed three times with tap water and submerged in hematoxylin solution for 12 minutes and rinsed with tap water. The slides were held for 1 minute in an ammonium hydroxide water solution (500 mL H_2O, 2 drops ammonium hydroxide), the pH of the water was adjusted to pH 9 with ammonium hydroxide, the slides were rinsed again in tap water. The slides were submerged in eosin stain for 90 seconds and rinsed with tap water at least 3 times or until there was no noticeable coloration of the rinse water. The slides were removed from the rinse water, inverted, and allowed to dry on the laboratory bench overnight. Once dry, the slides were mounted with Permount and allowed to dry. The mounted slides were then placed in a slide folder and allowed to dry completely for at least 3 weeks.

2.6 Western Blot

Lumpfish eye tissues were collected as previously described in section 2.1 by Dr. Robert Gendron and Dr. Hélène Paradis. Cell lysates for lumpfish retina, lumpfish rete mirabile and head kidney tissues were prepared in RIPA2++ lysis buffer (Table 2.1) as previously reported by our group (Paradis et al., 2008). Tissue samples were homogenized in the RIPA2++ buffer and then agitated at 4^0C for 20 minutes. The cell lysates were then clarified by centrifugation at 10,000 g at 4^0C. The protein extract supernatant was collected and stored at -

80^0C for future protein quantification. Protein concentration was determined by using a spectrophotometer. Bovine serum albumin (BSA) was used as the control and the Bradford Bio-Rad Protein Assay Kit (Mississauga, ON) was used to determine concentration. Sodium dodecyl sulfate polyacrylamide gel (SDS-PAGE) was completed as previously reported (Laemmli, 1970) with minor modifications optimized by the Gendron/Paradis laboratory. A 6.5% separating gel and a 3.5% stacking gel were used (Table 2.3). Prior to loading samples onto the gel all volumes of protein sample were adjusted to an equal volume with RIPA2++ buffer. Western blots were performed by loading desired amounts of protein onto the SDS-PAGE. Amounts of protein loaded on the gel varied depending on the level of expression of the protein of interest in each extract. These ranges of ug of protein (5 ug to 200ug) were loaded on the gel in a final volume of 35 ul. Molecular weight markers (5-245 kDa, BLUelf Prestained Protein Ladder, Froggabio) were used as the molecular weight reference. The gel apparatus was then connected to a power supply and set at 3-4 mA and 100V limit and left to run overnight. Prior to transfer the gel was soaked in cold transfer buffer without methanol (16.64g Tris Base, 79.30g Glycine, 4L dH$_2$O) for 15 minutes. The gel was placed on 0.2 um Nitrocellulose membrane (BioRad Laboratories) and was then set between 3MM Whatman paper and the transfer apparatus. The transfer tank was filled with cold transfer buffer containing methanol (16.64g Tris Base, 79.30g Glycine, 4L dH$_2$O, 990mL MeOH). The transfer apparatus was then placed in the transfer tank and the proteins from the gel were set to transfer for 30 minutes at 40 V, after 30 minutes the voltage was increased to 45 V for 2 hours. Fresh ECL block was prepared as previously described in section 2.4, and the membrane was placed in a sealed glass dish with ECL block at 55^0C with 70 rpm agitation for 1 hour to block non-specific binding. For protein detection, membranes were incubated overnight at room temperature with primary antibody (Table 2.4) in 2% ECL block/Tris-Buffered Saline

Tween-20 (TBST)/0.01% NaN$_3$. Following primary antibody incubation, the membrane was washed in tris buffered saline + Tween 20 (TBST) 7 times for 5 minutes each. Proceeding the final wash, the membranes were incubated with secondary HRP conjugated antibodies (Table 2.4) in 2% ECL block in TBST for 2 hours at room temperature. Clarity (BioRad Laboratories) and Lumiglo (GE Healthcare; KPL) substrates were used for chemiluminescent detection analysis. To develop the HRP reaction excess TBST was removed from the membranes using two pieces of 3MM Whatman paper. The membranes were placed on plastic wrap and the specific substrate was pipetted onto the membrane. The membranes were allowed to incubate with the substrate for 1 minute for Lumiglo substrate or 5 minutes for Clarity substrates. After substrate incubation, excess substrate was absorbed using 3MM Whatman paper and the membranes were covered in plastic wrap and flattened into a cassette. A Kodak Gel Logic 2200 imaging system and the Carestream computer software program were used to expose membranes for chemiluminescence and capture representative western blot images. RF/6A retinal endothelial cells and human umbilical vein endothelial (HUVEC) cell line samples previously cultured in the Gendron/ Paradis lab (Gendron et al., 1996; Gendron, Good, et al., 2001) were used as positive controls for CLIC2 Western blot analysis. RF/6A retinal endothelial cells were used as a positive control cell lines for ZO-1 Western blot. Daudi Burkitt's Lymphoma cell line a kind gift from Dr. Shelia Drover (Memorial University) was used as a negative control for ZO-1. mouse endothelial cell line IEM (Gendron et al., 1996) were used as a positive control for CD10.

	30% acrylamide (2.66% bis acrylamide)	4X Resolving Gel buffer pH 8.8	H_2O	Temed	10% Ammonium persulfate (APS)
Separating Gel (6.5%)	3.0 mL	3.75 mL	8.0 mL	12 ul	110 ul
Stacking Gel (3.5%)	30% acrylamide (2.66% bis acrylamide	4X Resolving Gel buffer pH 6.8	H_2O		
	5.6 mL	12 mL	30.4 mL		

Table 2.3: Gel Components

Antigen	Host	Antibody	Clone	Primary or Secondary Ab	Isotype	Ab Dilution	Source and Product #
CD10	Rabbit	Monoclonal	SP67	Primary	IgG	1/1000	ab227640, abcam
CD45	Seabass	Monoclonal	DLT22	Primary	IgG	1/20	Scapigliati group[†], University of Tuscia, Italy
CLIC2	Rabbit	Monoclonal	EPR6494	Primary	IgG	1/500	ab175230, abcam
ZO-1	Mouse	Monoclonal	ZO1-1A12	Primary	IgG	1/1000	WA316684, Invitrogen
Tubulin	Mouse	Monoclonal	DM1A	Primary	IgG	1ug/ml	9026, Sigma
Mouse	Goat	-	-	Secondary (HRP)	IgG	1/7500	W402B, Promega
Rabbit	Goat	-	-	Secondary (HRP)	IgG	1/7500	W401B, Promega

Table 2.4 Primary and Secondary Antibodies Used in Western Blotting
[†](Marozzi et al., 2012)

2.7 Quantitation and Statistical Analysis

Each developmental stage had n ≥ 3 independent biological replicates. Average stain

intensity of CLIC2 and ZO-1 of the vasculature of the rete mirabile was performed on each

specimen from larval, juvenile and adulthood developmental stages. For each rete mirabile a 40X

high power focus (hpf) image of the strongest staining area was obtained using Openlab 5.5

microscopy software and a LEICA DM 4000B microscope. Each image was individually

uploaded to ImageJ software for analysis. Five stain intensity line measurements of the strongest

staining areas of the rete mirabile and five background line measurements were obtained from

each image using the freehand line tool in ImageJ. The background line measurements were

taken from the red blood cells within the rete mirabile vasculature of each image. The stain

intensity red, green and blue values for each freehand line was obtained from ImageJ software

and inserted into a Microsoft Excel Document where the ratio of red over green values and all

sequential calculations was determined. For each line measurement for each image the average,

the standard deviation and standard error were calculated using the ratios determined. The

overall averages of the average stain intensity, overall average standard deviation and overall

average standard error was determined for stain intensity and background. Background staining

was then subtracted from overall staining intensity.

Quantification of the frequency of CD45 staining cells within the rete mirabile of

lumpfish over a developmental time course was conducted. The size of the rete mirabile of larval

and juvenile lumpfish was very small in comparison to the size of the adult rete mirabile. Due to

the small size, an appropriate high-power focus (hpf) image of the rete mirabile that fits the

entirety of the camera view is unachievable. The rete mirabile from the larval and early juvenile

stages were quite small in width but long in length, to fit the most rete mirabile per field of view

the highest possible power the images could be captured at was 20X objective. Representative

images of the rete mirabile from larval, juvenile and adulthood developmental stages were

obtained and individually processed using ImageJ. The TIFF image files were uploaded to

ImageJ then using the polygon selection tool an outline was drawn of the rete mirabile. Once the

entire rete was outlined the area was analyzed in ImageJ by clicking 'Analyze' then 'Measure'

and the areas were recorded in an excel file. To obtain the most accurate measurement, each rete

mirabile was outlined and analyzed three times. The average of the three area measurements was

used to determine appropriate area size for each rete image. The number of CD45+ cells were

manually counted, and the number of stained cells was also recorded in the excel file. To account

for any potential bias, two other graduate student researchers also counted the CD45+ staining cells and recorded their findings. CD45+ cell counts were performed on slides that were coded such that the origin of sections was not known. The images were renamed, randomly naming the image a letter, and removing all identifying descriptors. This process was conducted on each rete mirabile image from each developmental stage. Based on this information a ratio was developed to compare the number of positively staining cells most accurately in each rete mirabile.

Statistical analysis was conducted for the data from the CLIC2 and ZO-1 stain intensity of the rete mirabile vasculature and frequency of CD45+ stained cell quantitation. Graphs depicted within this thesis were created in Microsoft Excel and were presented with ± standard error of the mean (SEM). Each developmental stage, larval (0-50dph), juvenile (50-250dph), and adulthood (250+dph) had n ≥ 3 independent biological replicates unless otherwise stated. Graph Pad Prism v.9.3.1 was used to perform the analysis of variance (ANOVA) between the three developmental stages. Statistical significance was determined by running a Tukey's multiple comparisons test where $p < 0.05$.

Chapter 3: Results

3.1 Protein BLAST Analysis

Analysis of expression of CD10, CD45, CLIC2, PCNA and ZO-1 was performed using the antibodies indicated in Table 2.1 for immunohistochemistry and Table 2.2 for Western blot. To determine potential cross reactivity of each antibody with *C. lumpus*, *C. lumpus* sequences for CD10, CLIC2, PCNA and ZO-1 were compared to human. As the anti-CD45 antibody was raised against sea bass, the *C. lumpus* CD45 protein sequence was compared to the CD45 protein sequence of sea bass that has previously been determined by the Scapigliatti group (Marozzi et al., 2012). Protein BLAST was conducted to determine homology between *C. lumpus* and *Homo sapiens* or *Dicentrarchus labrax* protein sequence. Determining sequence identity provided the opportunity to anticipate if the protein sequences of the markers of interest were homologous enough to cross react with the *C.* lumpus proteins. *C. lumpus* ZO-1 showed 78.41% identity to *Homo sapiens* ZO-1 protein sequence. *C. lumpus* CLIC2 showed 71.81% identity to *Homo sapiens* CLIC2 protein sequence. *C. lumpus* CD45 showed 93.89% identity to *Dicentrarchus labrax* CD45 protein sequence. The epitope for the antibodies were identified from each antibody specification sheet and another BLAST search was conducted. The epitope of each antibody, except for CD45, was of human origin. The CLIC2 antibody epitope corresponds to amino acids 1- 100 and was found to have an 80% identity. The ZO-1 antibody epitope corresponds to amino acids 334 to 634, this epitope was found to have an 83% identity. The Gendron/ Paradis lab determined the homology of *C. lumpus* CD10 to *Homo sapiens* CD10 prior to the commencement of my studies. It was found that human CD10 is 60% identical to the lumpfish CD10 sequence (Gendron et al., 2020). Bioinformatics for the PCNA antibody was previously conducted by the Gendron/ Paradis lab. PCNA sequences of *Dano rerio (D. rerio)*

and *Salmo salar* were compared to human PCNA sequence. Both *D. rerio* and *Salmo salar* demonstrated greater than 90% identity to the human PCNA sequence (Ahmad et al., 2019). As the lumpfish genome is now readily available, a BLAST search was conducted using the human PCNA protein sequence against lumpfish. The PCNA antibody epitope corresponds to amino acids 1 to 261 full length PCNA. It was found that the human PCNA sequence had a 91.19% identity to the lumpfish sequence. It was found that the sequences had sufficient homology with *C. lumpus* of greater than 80% identity.

3.2 Western blot analysis of CD10, CD45, CLIC2 and ZO-1 protein in lumpfish eye tissues

Western blot analysis was conducted to confirm the location of expression for CD10, CD45, CLIC2 and ZO-1 that was indicated by the immunohistochemistry findings. Western blot analyses were performed on adult lumpfish retina and lumpfish rete mirabile tissues with different mammalian cell lines used as positive or negative controls (Fig. 2). For all Western blots tubulin was used as the loading control. Using SP67 and DLT22 mAb, Western blot analysis of CD10 and CD45 protein in tissue lysates of lumpfish retina and lumpfish rete mirabile (Fig. 2 A) revealed that CD10 is detectable in the lumpfish retina and not present in the lumpfish rete mirabile. CD45 was strongly detected in the lumpfish rete mirabile but does not seem to be present in the lumpfish retina. While little to no expression of CD10 was present in the rete mirabile and CD45 was seen to have little to no expression in the lumpfish retina.

Using EPR6494 mAb, Western blot analysis of CLIC2 protein in tissue lysates of lumpfish retina and lumpfish rete mirabile (Fig. 2 B) revealed that CLIC2 is detectable in both the lumpfish retina and lumpfish rete mirabile. Lastly, using ZO-1-1A12 mAb, Western blot

analysis of ZO-1 protein in tissue lysates of lumpfish retina and lumpfish rete mirabile (Fig. 2 C) revealed ZO-1 was detectable in lumpfish rete mirabile.

All markers were observed to have expected molecular weights. The predicted molecular weight of human CD10 was 86 kDa, and the lumpfish 88 kDa, the molecular weight observed was determined to be 100 kDa. This was expected as the observed molecular weight may be because of post translation modifications or glycosylation. The antibody used for CD45 was developed against sea bass and the molecular weight had been previously described (Marozzi et al., 2012). The expected molecular weight of CD45 was 180 kDa as that was the observed molecular weight in sea bass (Marozzi et al., 2012). There were two protein bands detected in the Western Blot, one band migrating just below 253 kDa and the other above the 180 kDa marker. The observed molecular weight of CLIC2 was the same as the predicted molecular weight of 29 kDa. The predicted molecular weight of human ZO-1 is 195 kDa, the molecular weight of lumpfish ZO-1 determined from Western blot was 236-248 kDa. In the literature, human ZO-1 has been observed to have a molecular weight of 210-225 kDa (Gumbiner et al., 1991; Stevenson et al., 1986). Differences in the molecular weight observed from the western blot I conducted may be due to post translation modifications or glycosylation.
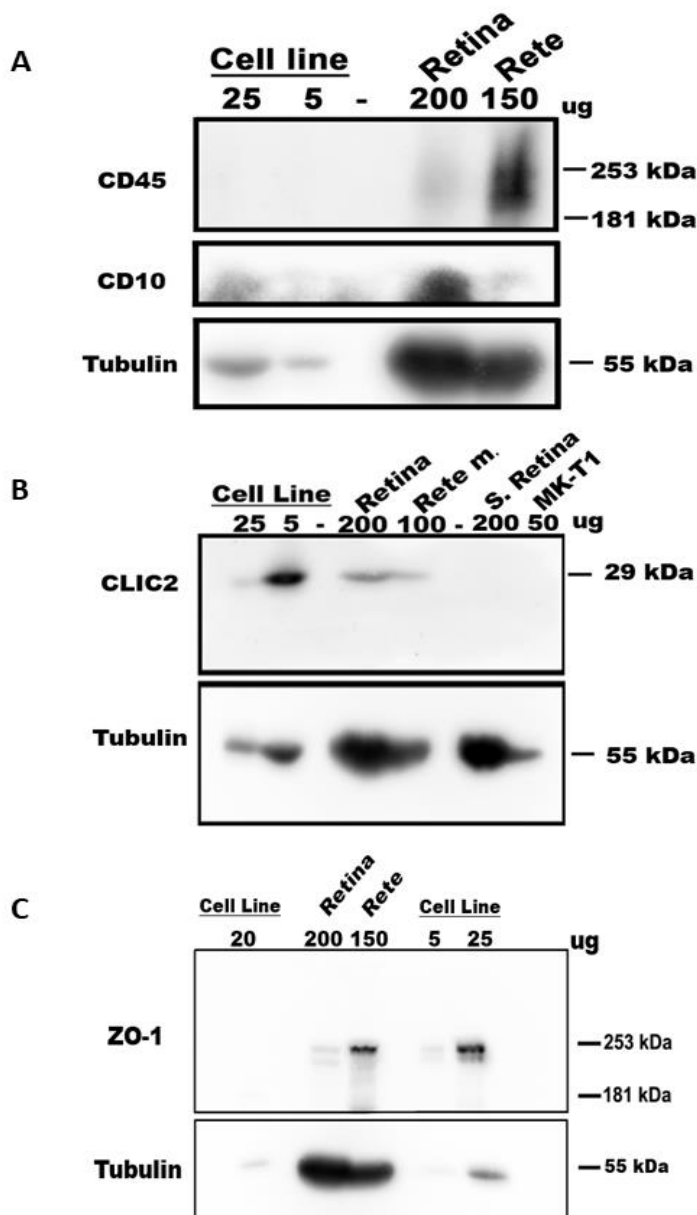
Figure 2. Western blot analysis of CD10, CD45, CLIC2 and ZO-1 protein in lysates of lumpfish eye tissues. A-C, Representative western blots of lumpfish retinal and rete mirabile lysates were performed using the indicated antibodies. For all western blots, tubulin is detectable in all protein lysates and serves as a loading control. **A**, CD45 protein is detectable in the lumpfish Rete m. (rete mirabile) tissue while CD10 protein is detectable in lumpfish retina. IEM cell line (5 and 25ug) serves as a positive control for CD10. CD45 is not detected in these cells. **B**, CLIC2 protein is detectable in lumpfish retina and rete mirabile. RF/6A retinal endothelial cells (25ug) and human umbilical vein endothelial cells (5ug) serve as positive control cell lines for CLIC2. CLIC2 was not detected in the smelt retina (S. Retina) or in MK-T1 cell line (50 ug) (Gendron, Liu, et al., 2001). **C**, ZO-1 protein is detectable in lumpfish retina and rete mirabile tissues. RF/6A retinal endothelial cells (5 and 25ug) serve as a positive control for ZO-1. ZO-1 is not detectable in Daudi cell line (20ug) and is used as a negative control.

46

3.3 CD10 expression in the developing lumpfish eye

Lumpfish head kidney and human tonsil was previously used as positive control tissue for CD10 IHC by the Gendron/ Paradis lab (Gendron et al., 2020) as they exhibit sufficient levels of CD10. CD10 was present in the basal cells of the renal tubules and in cells of the follicular region of the head kidney and a large number of CD10+ cells were also present in the human tonsil, as expected (Gendron et al., 2020).

CD10 immunohistochemistry was performed on *C. lumpus* whole larvae, head and eye paraffin wax sections from 20, 48, 85, 118, 150, 263 and 606 dph lumpfish. CD10 was present in the lumpfish retina as expected (Fig. 3). IHC revealed that CD10 was expressed in the inner plexiform layer as well as in a distinctive banding pattern in the areas of the cell bodies of the rods and cones and in the outer plexiform layers (Fig. 3 A, B, C). CD10 staining seems to appear much stronger in the retina of larvae than in the juvenile and adult specimens (Figure 3 A-C all arrowhead comparisons). Hematoxylin and eosin (H&E) staining of serial adult (Fig. 3 D) and larval (Fig. 3 E) sections show the layers of the retina (Fig. D-E). H&E images were used to help determine the location of CD10 expression.

Immunohistochemistry also revealed that CD10 was expressed in the limbus of *C. lumpus* eye (Fig. 4). Staining levels of CD10 in the limbus appear to remain the same throughout development as stain intensity remains relatively similar throughout each developmental stage (Fig. 4 A-D). Hematoxylin and eosin (H&E) staining of serial larval (Fig. 4 F), juvenile (Fig. 4 G) and adult (Fig. 4 H) sections indicates the limbus and surrounding ocular structures including the anterior chamber, iris (Fig. 4 G) and the retractor lentis muscle (Fig. 4 H).
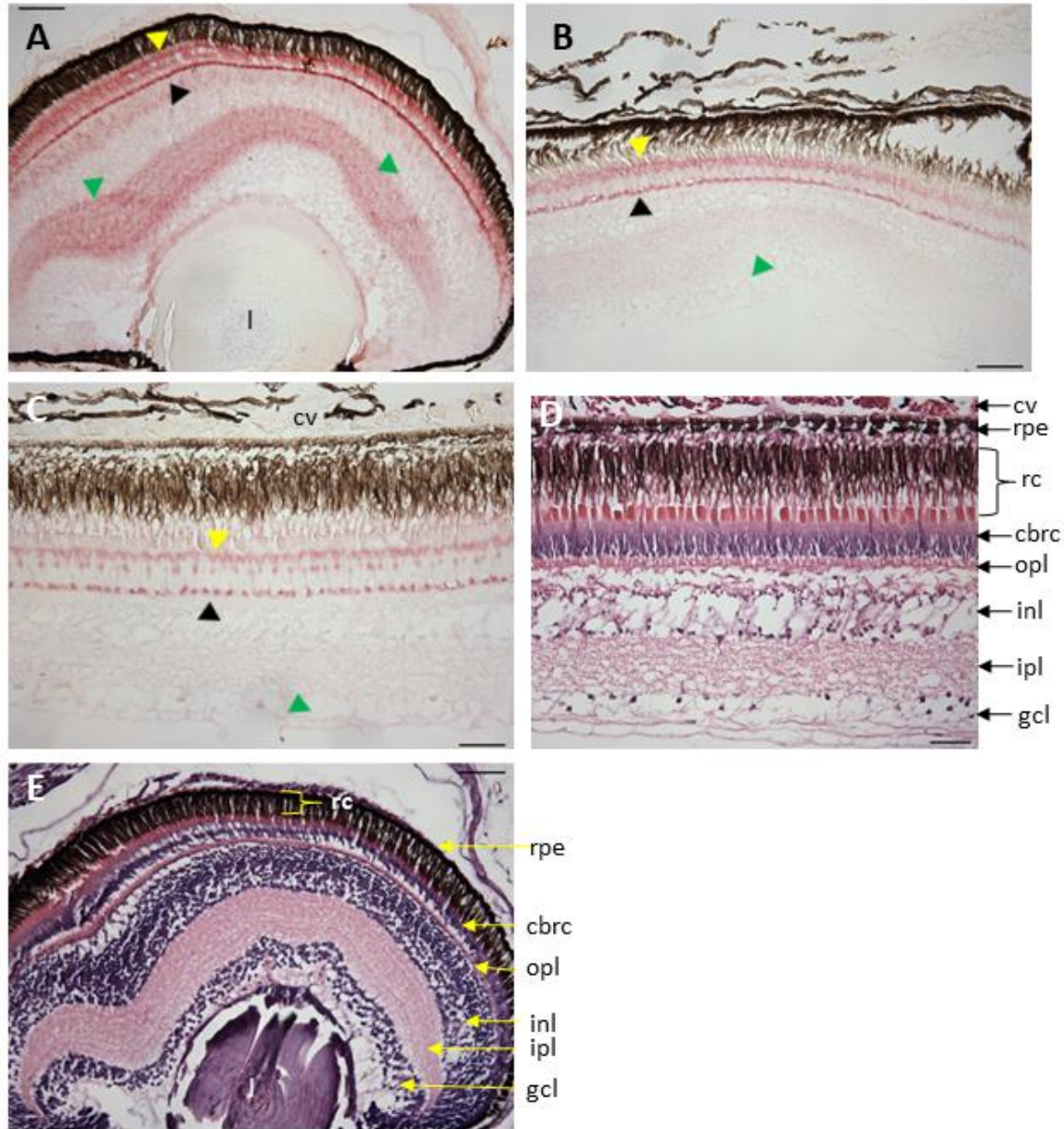
Figure 3. CD10 expression in lumpfish retina. A-C Immunohistochemistry (IHC) for CD10 expression (pink/ red stain). Representative IHC images of lumpfish retina through larval (A), juvenile (B) and adult (C) developmental stages. **A**, Retina of larval (20 dph) lumpfish. CD10 expression is present in the outer plexiform (black arrowheads) and inner plexiform (green arrowheads) layers of the retina. CD10 is also present in the photoreceptor components (yellow arrowheads). **B**, Retina of juvenile (118 dph) lumpfish. CD10 expression is present in the outer plexiform layer (black arrowheads) and photoreceptor components (yellow arrowheads). Expression of CD10 appeared lower in the inner plexiform layer (green arrowheads) of juvenile lumpfish relative to larvae. **C**, Retina of adult (606 dph) lumpfish. CD10 expression is present in the outer plexiform layer (black arrowheads) and photoreceptor components (yellow arrowheads). CD10 expression in the inner plexiform layer (green arrowhead) appears less intense than juvenile and larval lumpfish. **D**, Representative adjacent histological section of an

adult lumpfish (606 dph) retina. Choroid vasculature and retinal layers of adult lumpfish (choroid vasculature (cv), retinal pigment epithelium (rpe), rods and cones (rc), cell bodies of rods and cones (cbrc), outer plexiform layer (opl), inner nuclear layer (inl), inner plexiform layer (ipl), ganglion cell layer (gcl)). **E**, Representative adjacent histological section of a larval lumpfish (20 dph) whole eye. Presumptive layers of larval retina (choroid vasculature (cv), retinal pigment epithelium (rpe), rods and cones (rc), cell bodies of rods and cones (cbrc), outer plexiform layer (opl), inner nuclear layer (inl), inner plexiform layer (ipl), ganglion cell layer (gcl)). All images taken at 20X objective and scale bar 50 um. **A-C** larvae n= 13 individuals (23 eyes), juvenile n= 3 individuals (10 sections), adult n= 3 individuals (6 eyes).
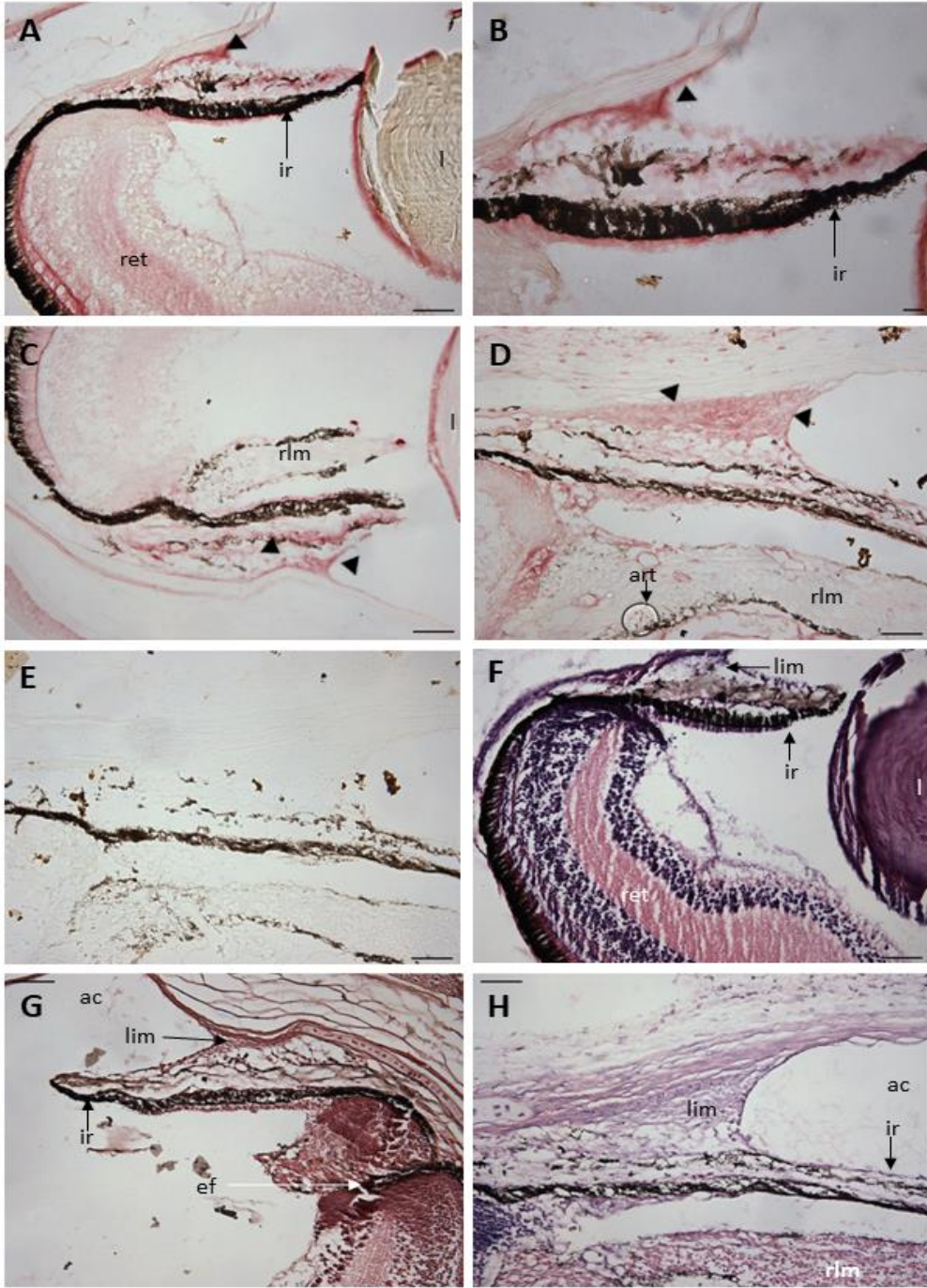
Figure 4. CD10 expression in limbus region of developing lumpfish eye. A-D,
Immunohistochemistry (IHC) for CD10 expression (pink/red stain). Representative IHC images
of lumpfish limbus over larval, juvenile and adult developmental stages. **A-B**, Limbus of larval
(48 dph) lumpfish. CD10 was found expressed in the limbus as indicated by the black
arrowhead. **C**, limbus of juvenile (85 dph) lumpfish. **D**, limbus of adult (263 dph) lumpfish. **A-D**,
Expression appeared to remain the same throughout development. **E**, Negative control image of
adult (263 dph) limbus showing no staining. **F-H**, Representative adjacent histological sections

of larval (48 dph) (**F**), juvenile (85 dph) (**G**), and adult (263 dph) (**H**) limbic (lim) regions. Other structures depicted are the anterior chamber (ac), iris (ir), retina (ret), embryonic fissure (ef) and retractor lentis muscle (rlm). **A** 20X objective and scale bar 50 um, **B** 40X objective and scale bar 25 um. **C-H**, 20X objective and scale bar 50 um. **A-E** Larvae n= 13 individuals (23 eyes), juvenile n= 3 individuals (10 sections), adult n= 3 individuals (6 eyes)

3.4 CD45 expression in the rete mirabile of the developing lumpfish eye

CD45 immunohistochemistry was performed on *C. lumpus* whole larvae, head and eye

paraffin wax sections from 20, 48, 85, 118, 150, 263 and 606 dph lumpfish. IHC revealed that

CD45 immunostaining was observed in leukocytic like cells in the rete mirabile of all age groups

as CD45 is a pan-leukocytic marker (Fig. 5 A-C). Hematoxylin and eosin (H&E) staining of

adjacent adult (Fig. 5 E) rete mirabile sections indicates the presumptive blood vessel wall and

red blood cell components of the rete vasculature. Following quantitation, it was determined that

the number of CD45 positive cells per millimeter (mm) square decreases from the juvenile age

(Fig. 5 G). Thus, this suggest that the number of CD45 expressing cells in the rete mirabile is

downregulated throughout development.

The head kidney is a known hematopoietic and immune organ, due to its immune

function lumpfish head kidney was used as a positive control tissue for CD45 immunostaining.

CD45 was found expressed on the periluminal aspect of the renal tubules and in the parenchyma
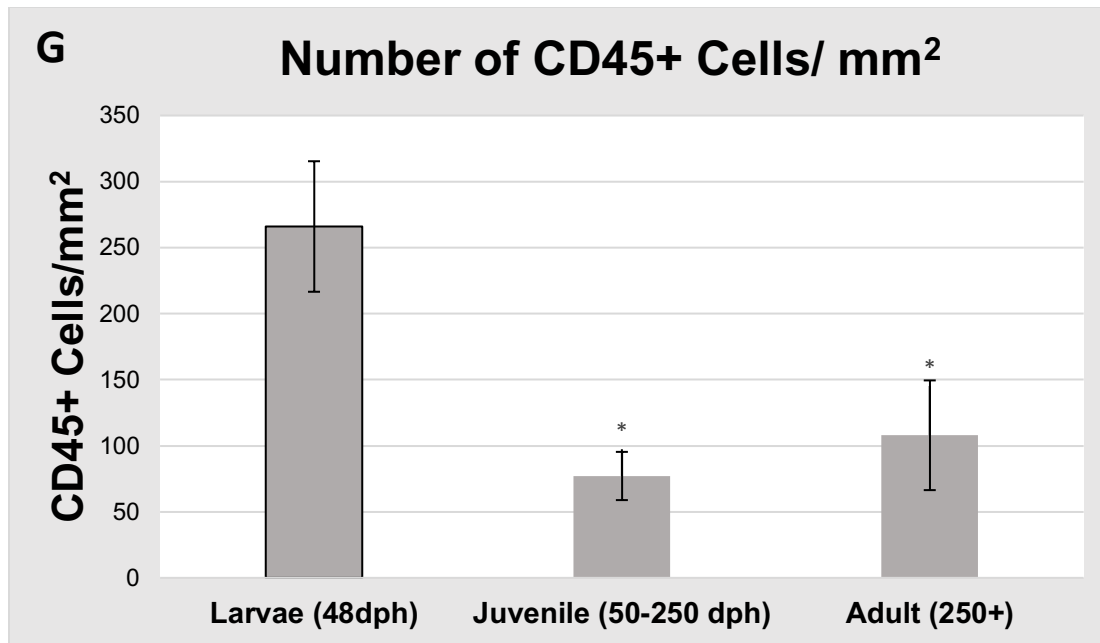
of the head kidney (Fig. 5 F).

51

G

Number of CD45+ Cells/ mm²
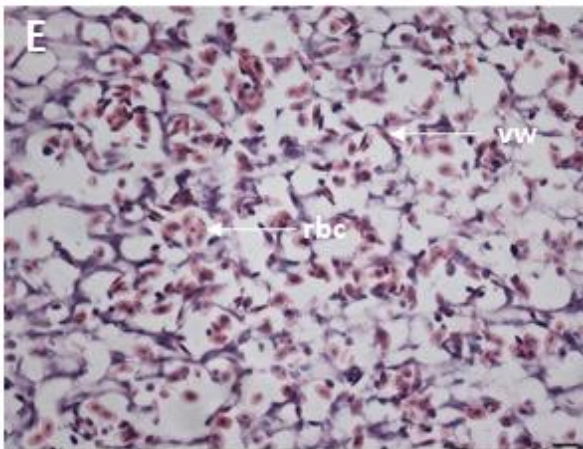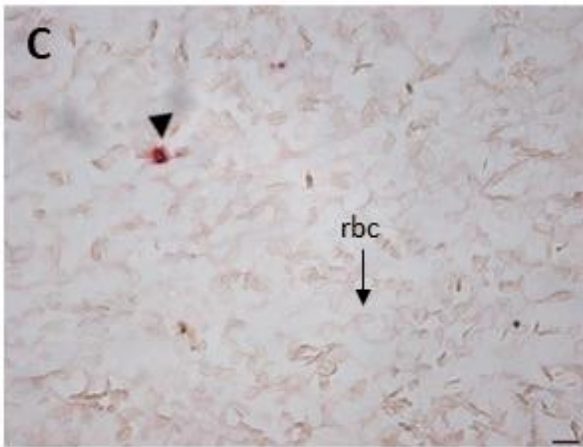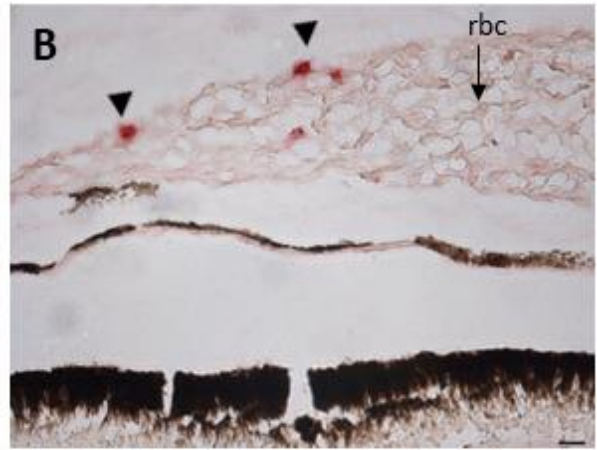
Figure 5. CD45+ cell expression in rete mirabile of developing lumpfish. A-C, Immunohistochemistry (IHC) for CD45 expression (red, punctate stain). Representative IHC images of lumpfish rete mirabile (rm) over larval, juvenile and adult developmental stages. **A**, Rete mirabile of larval (48 dph) lumpfish stained for CD45. CD45+ cells indicated by the black arrow heads. **B**, Rete mirabile of juvenile (85 dph) lumpfish stained for CD45. CD45+ cells indicated by the black arrow heads. Presumptive red blood cells (rbc) within blood vessels indicated by black arrow. **C**, Rete mirabile of adult (263 dph) lumpfish stained for CD45. CD45+ cell indicated by black arrowhead. Presumptive red blood cells (rbc) within blood vessels (black arrows). **D**, Negative control (no primary antibody) adult (263 dph) rete mirabile showing no reactivity. **E**, Representative adjacent histological section of adult (263 dph) rete mirabile depicting presumptive blood vessel walls (vw) and red blood cells (rbc) within the blood vessels. **F,** CD45 expression in adult lumpfish head kidney. CD45 expression in the periluminal aspect of the renal tubules and in the parenchyma (black arrowheads). **G**, Quantitation of CD45+ cells per unit area (mm²) in rete mirabile vasculature of larval, juvenile and adult specimens. Statistical significance was determined using one-way ANOVA and Tukey posthoc test (p≤0.05). Error bars represent standard errors, larvae n=4 individuals (5 eyes), juvenile n=3 individuals (6 eyes), adult n=2 individuals (3 eyes). **A-E**, 40X objective and scale bar 25 um.

3.5 CLIC2 expression in the developing lumpfish eye

CLIC2 immunohistochemistry was performed on *C. lumpus* whole larvae, head and eye paraffin wax sections from 20, 48, 85, 118, 150, 263 and 606 dph lumpfish. IHC revealed that CLIC2 was expressed in the rete mirabile (Fig. 6), iris (Fig. 7), tapetum (Fig. 6 A, Fig. 7 A) and retina (Fig. 6A, Fig. 7A). CLIC2 expression in the rete mirabile (Fig. 6 G) appeared to decrease

through development. Lumpfish head kidney was used as a positive control for CLIC2. CLIC2 expression was found in the basal cells of some renal tubules of the head kidney (Fig. 6 E). Quantitation (Fig. 6 G) as described in section 2.7, revealed that CLIC2 expression was downregulated from at least late larval stage (48 dph) and thereafter through development. Hematoxylin and eosin (H&E) staining of adjacent sections of adult (Fig. 6 F) rete mirabile indicated the presumptive blood vessel wall and red blood cell components of the rete mirabile. CLIC2 is also positively expressed by the tapetum (Fig. 6 A, Fig. 7 A).

Moreover, IHC also revealed that CLIC2 is expressed in the tips of the iris throughout development (Fig. 7). CLIC2 expression in the iris seems to remain the same throughout development (Fig. 7 A-C) as stain intensity seems to be relatively similar. Hematoxylin and eosin (H&E) staining of serial juvenile (Fig. 7D) iris and surrounding structures including the corneal epithelium, corneal stroma, anterior chamber, and limbus.
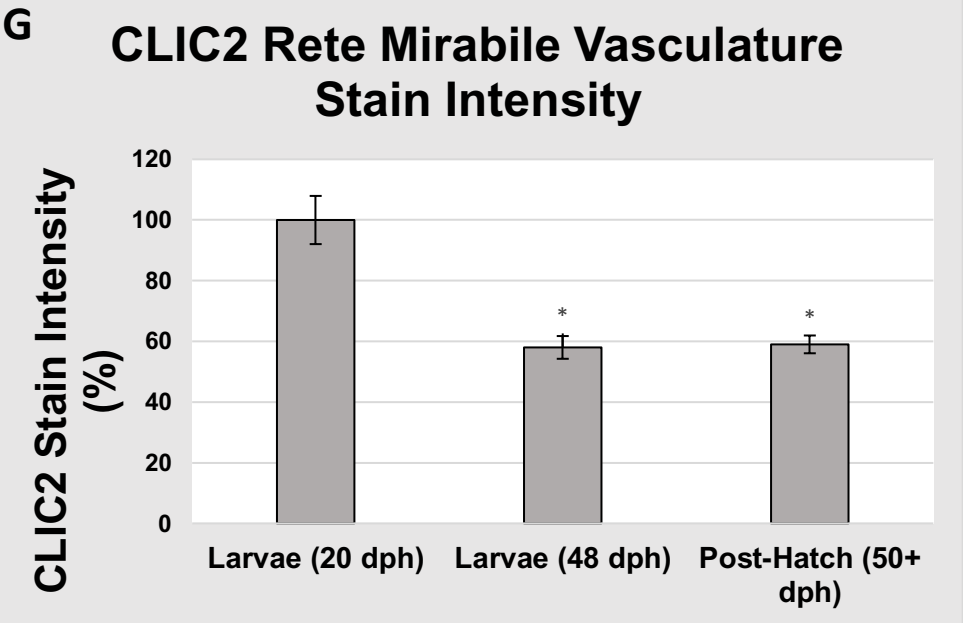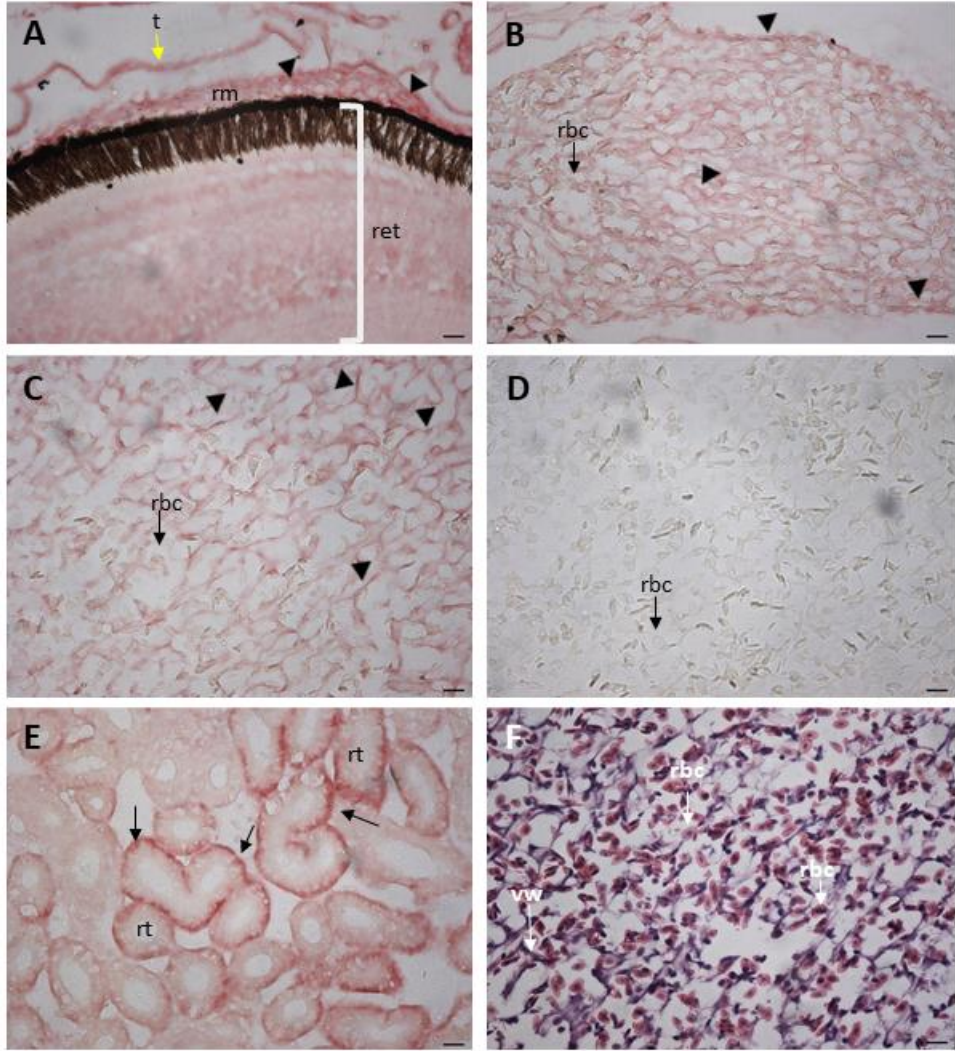
CLIC2 Rete Mirabile Vasculature Stain Intensity

Figure 6. CLIC2 expression in the rete mirabile of developing lumpfish. A-C, Immunohistochemistry (IHC) for CLIC2 expression (pink/ red stain). Representative IHC images of lumpfish rete mirabile (rm) over larval, juvenile and adult developmental stages. **A**, Rete mirabile of larval (20 dph) lumpfish positively expressed CLIC2 (black arrowheads). The tapetum (t) also positively expressed CLCI2 (yellow arrow). **B**, Rete mirabile of juvenile (118 dph) lumpfish positively expressed CLIC2 (black arrowheads). **C**, Rete mirbaile of adult (263 dph) lumpfish positively expressed CLIC2 (black arrowheads). **D**, Negative control (no primary antibody) adult (263 dph) lumpfish rete mirabile showing no reactivity. **E**, CLIC2 positive control tissue head kidney (263 dph). CLIC2 expression (black arrows) was found in the basal cells of some renal tubules (rt). **F**, Representative adjacent histological section of adult (263 dph) rete mirabile depicting the presumptive blood vessel walls (vw) and the red blood cells (rbc). **G**, Quantitation of CLIC2 expression of larvae versus post-hatch (50+ dph) rete mirabile vasculature by measuring average stain intensity (%). * Represents a statistical difference between larvae (20 dph) stain intensity. Statistical significance was determined using one-way ANOVA and Tukey posthoc test ($p \leq 0.01$). Error bars represent standard errors, larvae (20dph) n=6 individuals (12 eyes), larvae (48dph) n=6 individuals (10 eyes), post-hatch n=6 individuals (18 sections), 2 IHC replicates for each age. **A-F**, 40X objective and scale bar 25 um.
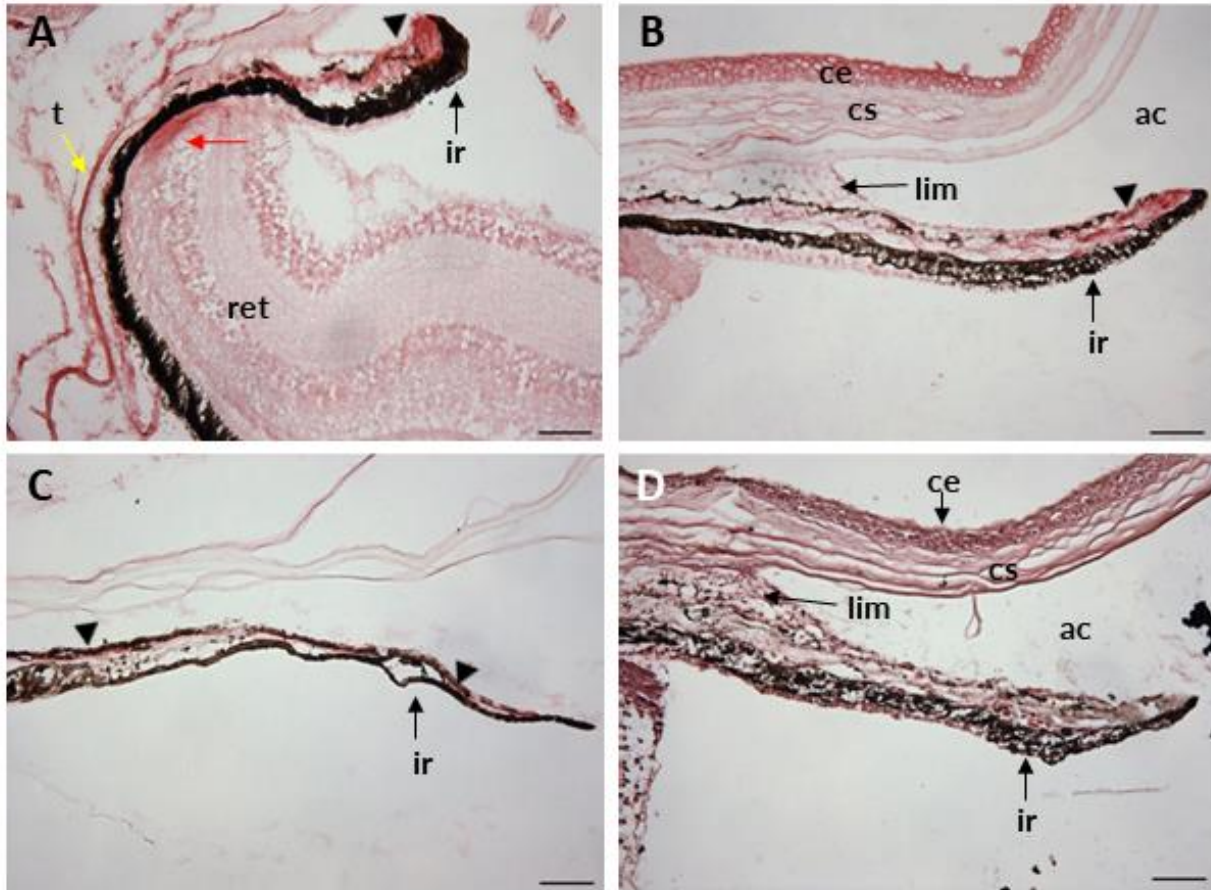
Figure 7. CLIC2 expression in the iris of developing lumpfish. A-C, Immunohistochemistry (IHC) for CLIC2 expression (pink/red stain). Representative IHC images of lumpfish iris (ir) over larval, juvenile and adult developmental stages. CLIC2 expression appeared to remain the same throughout development. **A**, Iris of larval (48 dph) lumpfish. CLIC2 was positively expressed in the iris (black arrowhead) as well as the tapetum (yellow arrow) and in the ciliary marginal zone of the peripheral retina (red arrow). **B**, Iris of juvenile (118 dph) lumpfish. CLIC2 was positively expressed (black arrowhead). **C**, Tip of iris of adult (606 dph) lumpfish. CLIC2 was positively expressed (black arrowhead). **D**, Representative adjacent histological section of juvenile (118 dph) lumpfish iris depicting the corneal epithelium (ce), corneal stroma (cs), anterior chamber (ac), limbus (lim) and the iris (ir). **A-C**, 20X objective and scale bar 50 um. **A-C** Larvae n= 14 individuals (22 eyes), juvenile n= 3 individuals (12 sections), adult n= 3 individuals (9 sections)
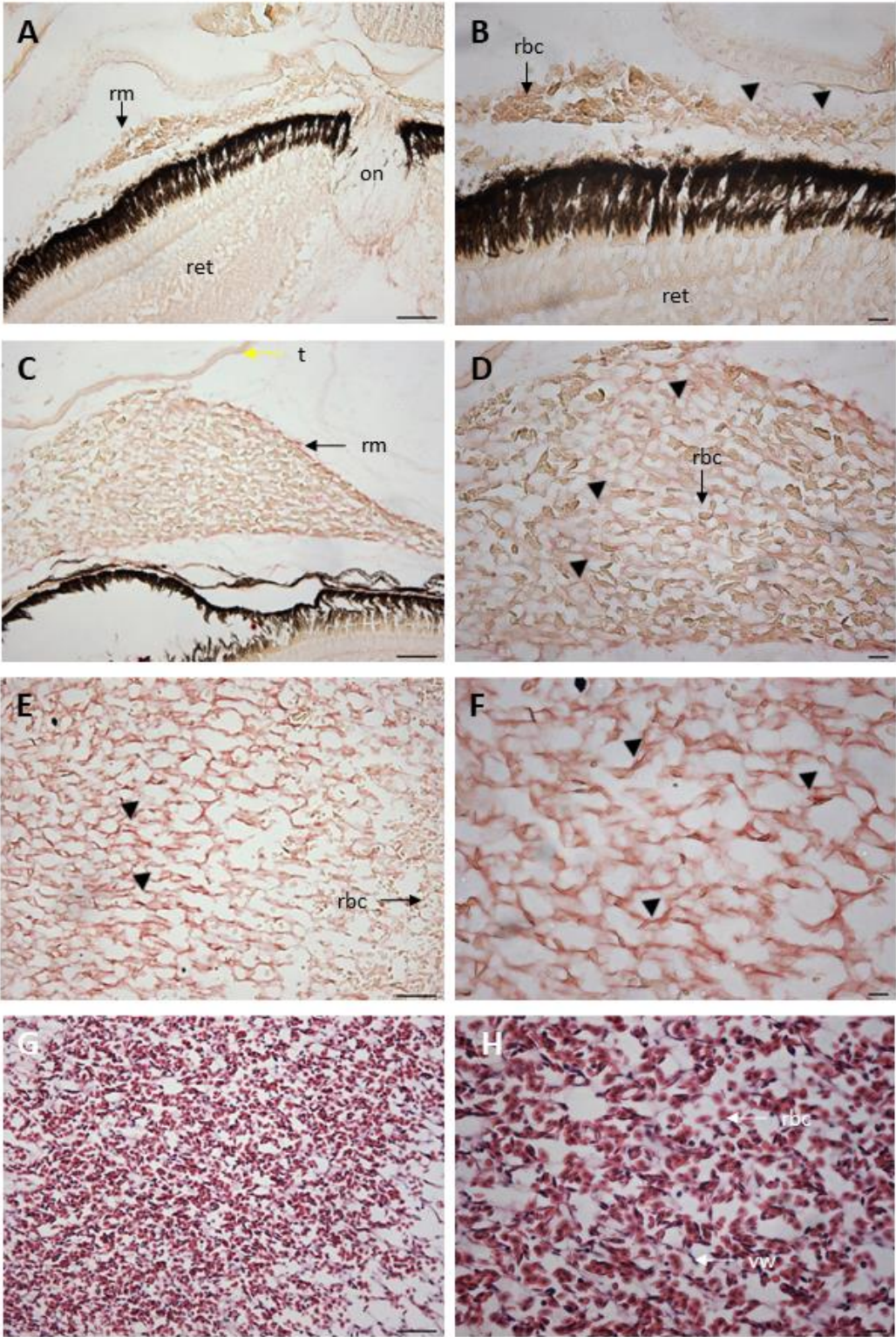
3.6 ZO-1 expression in the developing lumpfish eye

ZO-1 immunohistochemistry was performed on *C. lumpus* whole larvae, head and eye paraffin wax sections from 20, 48, 85, 118, 150, 263 and 606 dph lumpfish. IHC revealed that

ZO-1 was expressed in the rete mirabile (Fig. 8). ZO-1 expression in the rete mirabile appeared to increase through development (Fig. 8 A-F). Quantitation (Fig. 8 I) revealed that ZO-1 expression was upregulated through development. Hematoxylin and eosin (H&E) staining of adjacent sections of adult (Fig. 8 G-H) rete mirabile indicated the presumptive blood vessel wall and red blood cell components of the rete mirabile.

Expression of ZO-1 was also revealed by IHC in the limbus of *C. lumpus* eye. ZO-1 expression in the limbus appeared to remain similar throughout development (Fig. 9 A-D) as stain intensity was relatively the same through each developmental stage. Hematoxylin and eosin (H&E) staining of adjacent adult (Fig. 9 F) sections indicated the limbus and surrounding ocular structures including the anterior chamber, iris, and the retractor lentis muscle.

Mouse retina was used as a positive control for ZO-1 staining, the positive controls were used concurrently with the experiments, but the data is not shown.
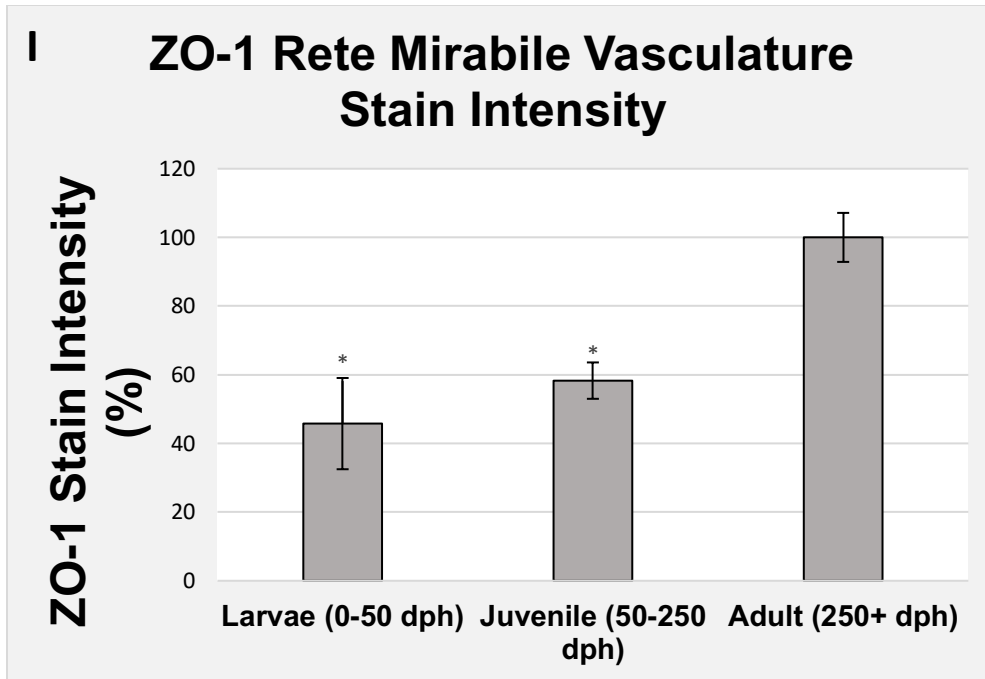
I

ZO-1 Rete Mirabile Vasculature Stain Intensity

Figure 8. ZO-1 expression in the rete mirabile of developing lumpfish. A-F, Immunohistochemistry (IHC) for ZO-1 expression (pink/red stain). Representative IHC images of lumpfish rete mirabile (rm) over larval, juvenile and adult developmental stages. ZO-1 expression appeared to gradually increase throughout development. **A, B**, Rete mirabile of larval (48 dph) lumpfish. Very low ZO-1 (black arrowheads) expression. **C, D**, Rete mirabile of juvenile (118 dph) lumpfish. ZO-1 (black arrowheads) expression appeared to increase relatively to larval stage. **E, F**, Rete mirabile of adult (606 dph) lumpfish. ZO-1 (black arrowheads) expression was increased relatively to earlier stages. **G, H**, Representative adjacent histological section of adult (606 dph) rete mirabile depicting the presumptive red blood cells (rbc) and the blood vessel walls (vw). **I**, Quantitation of ZO-1 expression of larvae, juvenile and adult rete mirabile presumptive vessel walls by measuring average stain intensity (%). * Represents statistical difference between adult (250+ dph) stain intensity. Statistical significance was determined using one-way ANOVA and Tukey posthoc test (p≤0.05). Error bars represent standard errors, larvae n=6 individuals (7 eyes), juvenile n=3 individuals (12 sections), adult n=2 individuals (3 eyes). **A, C, E, G**, 20X objective and scale bar 50 um. **B, D, F, H**, 40X objective and scale bar 25 um.
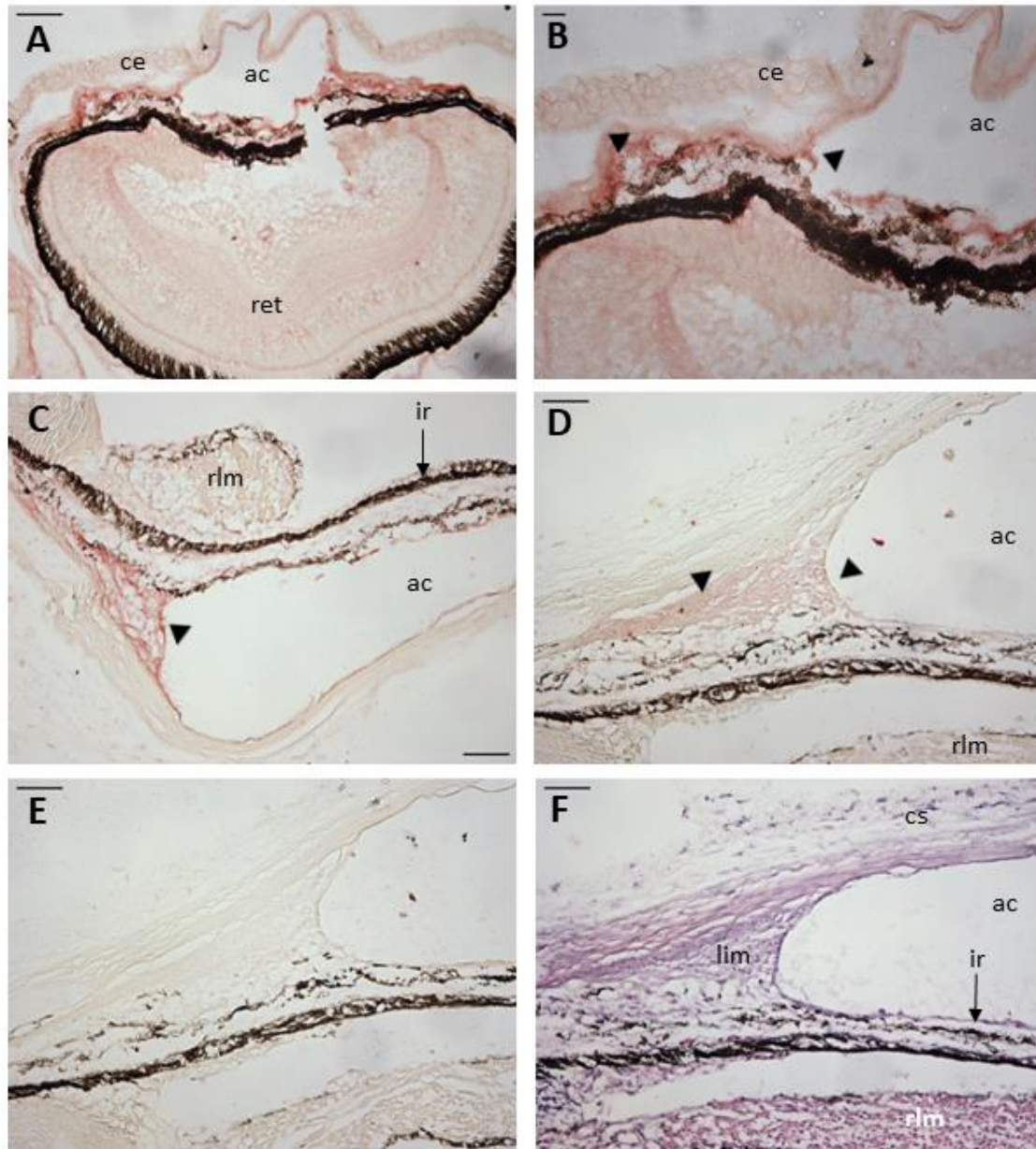
Figure 9. ZO-1 expression in limbus region of developing lumpfish eye. A-D,
Immunohistochemistry (IHC) for ZO-1 expression (pink/red stain). Representative IHC images
of lumpfish limbus over larval, juvenile and adult developmental stages. ZO-1 (black
arrowheads) staining levels appear to remain the same throughout development. **A, B**, larval (20
dph) lumpfish whole eye (**A**) and limbus region (**B**) can also see the corneal epithelium (ce),
corneal stroma (cs), anterior chamber (ac) and the retina (ret). **C**, limbus expressing ZO-1 (black
arrowhead) in juvenile (85 dph) lumpfish eye. The anterior chamber (ac), iris (ir) and the
retractor lentis muscle (rlm). **D**, limbus expressing ZO-1 (black arrowheads) in adult (263 dph)
lumpfish eye. **E**, Negative control adult (263 dph) limbus showing no reactivity. **F**,
Representative adjacent histological section of adult (263 dph) limbus (lim). Corneal stroma (cs),
anterior chamber (ac), iris (ir) and retractor lentis muscle (rlm) structures also represented. larvae

n= 14 individuals (16 eyes), juvenile n=3 individuals (12 sections), adult n=2 individuals (4 eyes) **A, C-F**, 20X objective and scale bar 50 um. **B**, 40X objective and scale bar 25 um.

## 3.7 Expression of CD10, CLIC2, PCNA and ZO-1 in the retractor lentis muscle vasculature of adult lumpfish

The adult (263 dph) lumpfish possessed a prominent retractor lentis muscle and the vasculature that supplies such muscle remained intact through embedding and sectioning procedures. However, it was difficult to find sections of this tissue in slides of earlier developmental stages or larger older adult lumpfish eyes as the vessels are very delicate. Therefore, IHC for various markers from the same adult (263 dph) specimen for the retractor lentis muscle region were performed. Other specimens, such as some of the juvenile specimens had retractor lentis muscle present but the vasculature was not. Other adult specimens, even of the same age, also did not have this tissue present. This could be due to variability in embedding and sectioning procedures. IHC revealed the expression of CD10 (Fig. 10 A), CLIC2 (Fig. 10 C) and PCNA (Fig. 10 E) within the presumptive blood vessel walls of the retractor lentis region. Interestingly, IHC revealed that ZO-1 (Fig. 10 G) was not expressed within the presumptive blood vessel walls of the retractor lentis area, the specimen that was incubated with ZO-1 antibody (Fig. 10 G) appears to be the same as the negative control (Fig. 10 H). Respective negative IHC controls for each marker are shown in Figure 10 B, D, F, and H. Hematoxylin and eosin (H&E) staining of adjacent adult (Fig. 10 I) sections indicated the retractor lentis muscle vasculature, the presumptive vessel wall and lumen, the presumptive red blood cells within the vessel as well as the retractor lentis muscle itself.
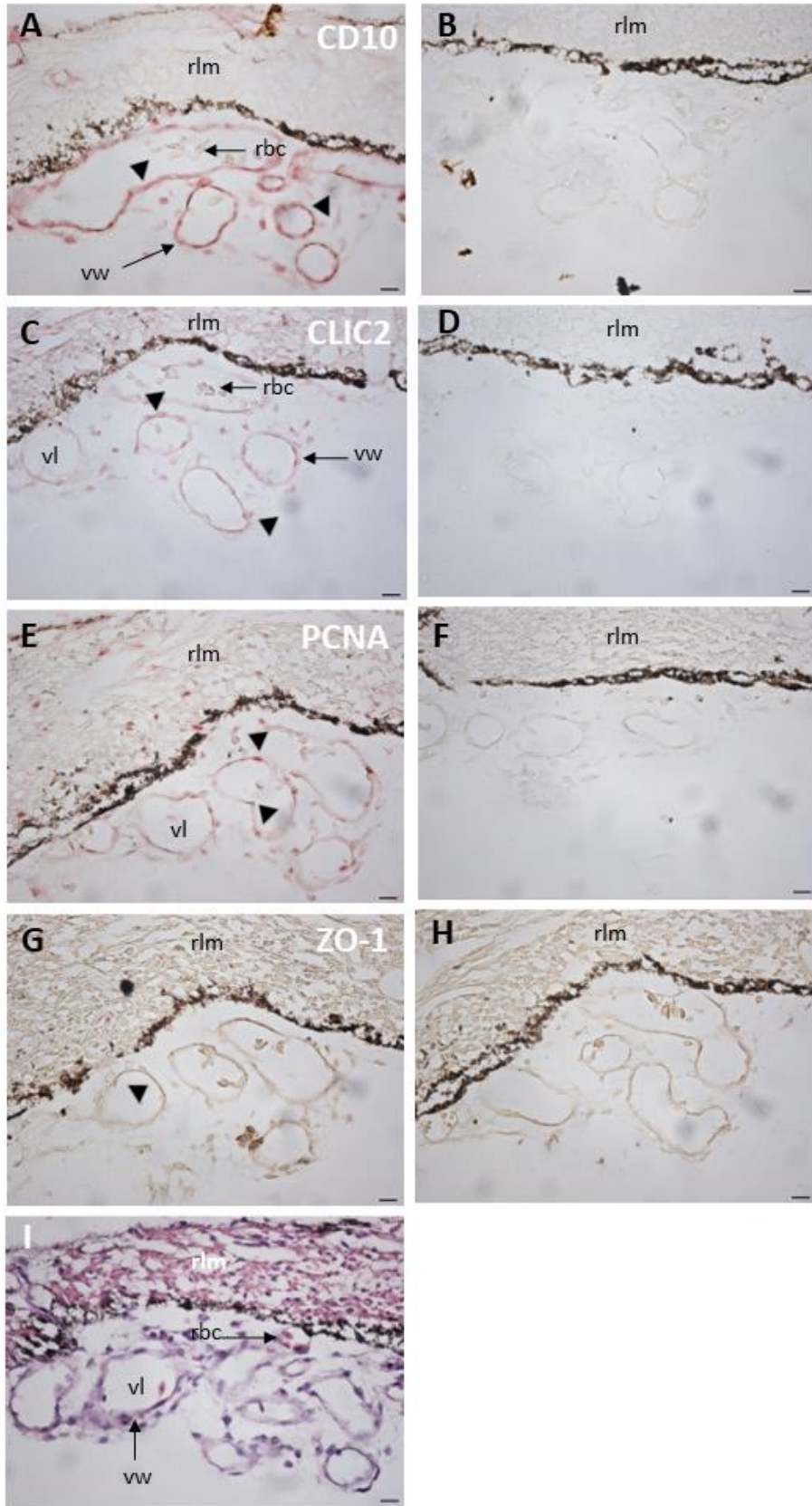
Figure 10. Expression of CD10, CLIC2, PCNA and ZO-1 in the retractor lentis muscle region of adult (263 dph) lumpfish eye. A, C, E, G, Immunohistochemistry (IHC) for CD10, CLIC2, PCNA and ZO-1 expression (pink/ red stain). Representative IHC images of lumpfish retractor lentis muscle area in adult (263 dph) lumpfish eye. **B, D, F, H**, Respective negative controls for CD10, CLIC2, PCNA and ZO-1 IHC results. **A**, Retractor lentis muscle presumptive vasculature stained for CD10. CD10 (black arrowheads) expression was seen in the presumptive blood vessels. **C**, Retractor lentis muscle presumptive vasculature stained for CLIC2. CLIC2 (black arrowheads) expression in the presumptive blood vessel walls of the vasculature. **E**, Retractor lentis muscle presumptive vasculature stained for PCNA (black arrowheads). **G**, Retractor lentis muscle presumptive vasculature stained for ZO-1. The vasculature appeared to be completely negative for ZO-1 expression as the negative control (**H**) was similar to the stained tissue (**G**). **I**, Representative adjacent histological section of the retractor lentis muscle presumptive vasculature of adult (263 dph) lumpfish eye. Identifying structures include the retractor lentis muscle (rlm), the presumptive blood vessel walls (vw) and lumen (vl), and the presumptive red blood cells (rbc). **A-I**, 40X objective and scale bar 25 um.

Chapter 4: Discussion

Lumpfish, a marine teleost found in the North Atlantic are becoming a species of interest for research as their use as a cleaner fish in aquaculture has increased over the past decade. Since the commercial importance of lumpfish in aquaculture began, the publication of the lumpfish genome has allowed for them to become an attractive model system. Previous work by the Gendron/ Paradis group examined the novel characteristics of lumpfish ocular tissues and found that many human eye structures are conserved in the lumpfish eye. However, lumpfish also possess various novel and exaggerated ocular structures unique to the species (Ahmad et al., 2019). I set out to examine the expression of various known markers of the vasculature and of the hematopoietic system, including barrier markers, within these structures.

I used immunohistochemical analysis to examine the pattern of expression and developmental regulation of CD10, CD45, CLIC2, PCNA and ZO-1 in the lumpfish ocular system. Western Blot analysis was used to explore the utility of these antibodies derived against mammalian or sea bass proteins to cross react with the lumpfish orthologue proteins. Histological sections of whole larvae, head, and eye specimens of lumpfish through various larval, juvenile and adulthood stages revealed that the various proteins of interest are developmentally regulated. To our understanding there is little to no knowledge of the expression of various proteins within the eye structures of lumpfish, nor is it known whether those proteins are developmentally regulated. Our results indicate that CD10, CD45, CLIC2, PCNA and ZO-1 are present within lumpfish ocular structures and suggest that these markers may be developmentally regulated.

CD10, a known marker for hematopoietic progenitor cells was found to be expressed in the lumpfish retina throughout development. CD10 was expressed in the inner plexiform layer as

65

well as in a distinctive banding pattern in the areas of the cell bodies of the rods and cones and in the outer plexiform layers. The patten of expression of CD10 is consistent with being present in the outer nuclear area of the retina representing the photoreceptor cell body. Through examination of the CD10 immunohistochemistry results, I observed that CD10 appeared to be downregulated in the inner plexiform layer of the lumpfish retina through development. Expression of CD10 appeared more intense in the inner plexiform layer of the retina of larval (20 dph and 48 dph) lumpfish than in the juvenile and adult specimens. The observed differences between larval and juvenile and adult lumpfish requires further investigation and quantification to determine whether the level of expression is influenced by a change in cell density. Further studies utilizing more advanced methods may be required to determine function and regulation.

The Gendron/ Paradis group found that the lumpfish eye continues to grow throughout adulthood, a characteristic that is well understood in teleosts (Ahmad et al., 2019). It is known that the teleost retina continues to grow through development as a result of the continual production of new retinal neurons (Otteson & Hitchcock, 2003).I found CD10 to be present in the lumpfish limbus. In mammals, the limbus is the border between the cornea and sclera and is the site of limbal stem cells (Gonzalez et al., 2018).The expression of CD10 in the limbus in lumpfish appeared to remain the same throughout development. CD10 was not detected in the ciliary marginal zone (CMZ) of the developing lumpfish retina, although PCNA (a proliferative marker) expression has been seen in this area (Ahmad et al., 2019). Thus, I expected to observe the presence of CD10 within the lumpfish retina and limbus as it is a hematopoietic progenitor cell marker. CD10 is significantly expressed in endothelial cells as previously described (Moneghini et al., 2020).

CD45 expression is found on all leukocytes in mammals (Marozzi et al., 2012). I chose to examine the expression of CD45 in lumpfish ocular tissues to provide an understanding into the lumpfish immune system and ocular homeostasis. CD45+ cells were largely found to be expressed in the lumpfish rete mirabile. Interestingly, I observed that CD45 expressing cells were downregulated in the rete mirabile of the lumpfish eye as development progressed as the amount of CD45+ cells per unit area decreased through adulthood. Though the development of the mucosal immune system in teleosts is not fully elucidated, it is known that at the time of hatching, the immune system is not fully functional (Chettri et al., 2012). Our results suggest that CD45 may play a role in immunologically protecting eye tissues until the mucosal immune system is fully developed.

CLIC2, a relatively novel marker with no homologous protein in murine models, was found to be expressed in lumpfish ocular tissues. As CLIC2 is not present in the murine genome, but has previously been identified in tilapia (Zeng et al., 2018), I set out to determine its expression in lumpfish. the lumpfish eye, CLIC2 was expressed in the vasculature endothelial cell of the rete mirabile as well as throughout the tips of the lumpfish iris. CLIC2 has not previously been explored by the Gendron/ Paradis group, following investigation into known areas of CLIC2 expression for a possible positive control, Zeng and colleagues (2018) found CLIC2 to be abundantly expressed in the kidney of tilapia. Thus, I used lumpfish head kidney as a positive control tissue for this research. Expression of CLIC2 within the lumpfish iris appeared to remain the same throughout development. Recently, Ueno and colleagues (2019) found CLIC2 to be highly expressed in normal blood vessel endothelia and was co-expressed with other tight junction proteins such as ZO-1 in non-cancerous human tissue. With this knowledge, the presence of CLIC2 in the presumptive endothelia of the rete mirabile vasculature was

expected. Following quantitation and statistical analysis on the intensity of CLIC2 staining within the rete mirabile, I found that CLIC2 is developmentally regulated. I found that CLIC2 expression the rete mirabile was highest at the early larval stage (20 dph) and expression decreased thereafter throughout the developmental timepoints observed. Interestingly, CLIC2 expression was observed in the lumpfish tapetum. Further studies of CLIC2 expression in the tapetum are required.

ZO-1, a tight junction scaffolding protein that is known to play a large role in vasculature endothelia was observed in various lumpfish ocular tissues. ZO-1 expression was observed in the limbus as well as the endothelial cells of the rete mirabile. ZO-1 expression in the limbus seems to remain the same throughout the developmental timepoints observed as stain intensity seems to be relatively similar through each developmental stage. Expression of ZO-1 was also observed in the presumptive endothelial cells of the rete mirabile. ZO-1 expression in the lumpfish rete mirabile increased throughout the developmental timepoints observed. This was an interesting finding as CLIC2, a protein thought to co-express with tight junction proteins such as ZO-1, was decreased in the rete mirabile throughout development.

I also observed expression of CD10, CLIC2 and PCNA within the presumptive endothelium of the retractor lentis muscle region while ZO-1 was not expressed. ZO-1 was not examined in this presumptive vasculature but was largely expressed in the vasculature of the rete mirabile. Whereas CD10 expression was seen in the presumptive vasculature of the retractor lentis muscle but not in the rete mirabile (not shown). I conducted immunohistochemistry on all developmental specimens and found that PCNA was expressed in the presumptive vessel wall of the retractor lentis muscle. The expression of PCNA in the endothelial cells was very interesting as endothelium is usually quiescent in mammals. The expression of CD10 and PCNA allow us to

question if the RLM vasculature could potentially be an area of stem cell niche and proliferation. Additionally, it is interesting that ZO-1 is highly expressed in the presumptive vasculature of the adult rete mirabile, but it is not expressed in the RLM presumptive vasculature. Because ZO-1 is not expressed that allows us to question if the vasculature of the RLM is potentially fenestrated or more permeable due to the absence of ZO-1, a known tight-junction protein. In mammals, the blood vessels of the ciliary body are known to be fenestrated and allow the passage of plasma and proteins (Zachary, 2017). If this vasculature is fenestrated, it may be used to not only supply the retractor lentis muscle with blood supply and nutrients but may also supply the lens with nutrients as they could diffuse through the fenestrated vessels and supply the lens.

Although lumpfish are gaining interest as model systems, to date there is little understanding of lumpfish development, specifically lumpfish ocular development. To our knowledge, our group is the only one to study lumpfish ocular systems and ocular development. I set out to characterize the expression of known markers of vascular and hematopoietic tissues associated with the development of the posterior ocular vascular versus hematopoietic tissue of lumpfish across a developmental time course. A better characterization of these lineages is needed to understand their role in ocular tissue development, homeostasis and stress response. Examining the expression of CD10, CD45, CLIC2, PCNA and ZO-1 also provided further basic knowledge on each of the proteins. Our study was successful in suggesting the expression of known vascular barriers and hematopoietic markers within the lumpfish eye tissue as well as examining regulation across the developmental time course.

This work provides the premise to conduct additional research into these markers, specifically to examine various signaling pathways and mechanisms of actions of these markers. The Wnt signaling pathway is linked to organogenesis during embryonic development, for

example in ocular development as it is required for normal eye development. This pathway is also known to regulate hematopoiesis (Chattopadhyay et al., 2019). Examining the signaling pathways will aid in further understanding the role that both immunological and barrier markers play in hematopoiesis.

Hematopoiesis is the process in which blood and its components are formed. It occurs during embryonic development and throughout adulthood in specialized tissues called primary lymphoid organs to produce and replenish the blood system (Jagannathan-Bogdan & Zon, 2013). Embryonically in mammals, hematopoiesis begins in the yolk sac and transitions into the liver temporarily before finally establishing definitive hematopoiesis in the bone marrow and thymus (Jagannathan-Bogdan & Zon, 2013). However, when hematopoiesis occurs outside of bone marrow the process is termed extramedullary hematopoiesis (EMH). EMH in mammals can occur in postnatal life to compensate for inadequate bone marrow hematopoiesis (Kim, 2010; Yamamoto et al., 2016). Prenatally, there are many sites of hematopoiesis, one of which is the ocular choroid vasculature. In a study by Arredondo and colleagues (2008) observing the ocular findings in pediatric deaths under 2 years of age, between 1994 and 2004, it was found that in many of the infants studied, EMH frequently occurred in the choroid (Arredondo et al., 2008). EMH present in the choroid vasculature of the mammalian eye proves interesting as not much is currently known about extramedullary hematopoiesis in ocular tissue. The choroid vasculature in mammals provides blood to the posterior retina (Kolb, 2012). The role of ocular vascular structures in response to stressors and hematopoietic mechanisms remains largely unstudied. In a study by Hasegawa and colleagues (2007) it was suggested that in humans the choriocapillaris is formed by a process called hemo-vasculogenesis. This is a process of vascular formation where new blood vessels and cells develop simultaneously within an embryo from a common precursor

called a hemangioblast (Hasegawa et al., 2007). This poses a potential developmental link between vasculature and hematopoiesis.

A better understanding of ocular extramedullary hematopoiesis could provide insight into relationships between the ocular vascular and hematopoietic systems and how these systems respond to stress. In teleosts, the CMZ is known to constantly regenerate and produce new stem cells, acting as a site of EMH. Lumpfish possess exaggerated ocular structures that could allow for them to be good models of extramedullary hematopoiesis. Continued studies of EMH in the lumpfish eye may be important for understanding ocular tissue development and hematopoiesis in a broader set of species, including humans. In this study, known immune and hematopoietic cell markers, CD10 and CD45 and barrier markers ZO-1 and CLIC2 were examined over a developmental time course in the lumpfish eye. In doing so, I characterized the expression of these markers to develop our understanding their role in ocular tissue development, homeostasis and immune responses.

References

Ahmad, R., Paradis, H., Boyce, D., McDonald, J., & Gendron, R. L. (2019). Novel
characteristics of the cultured Lumpfish *Cyclopterus lumpus* eye during post-hatch larval
and juvenile developmental stages. *Journal of Fish Biology*, *94*(2), 297–312.
https://doi.org/10.1111/jfb.13892

Ali, M. A. (Ed.). (1975). *Vision in Fishes: New Approaches in Research*. Springer US.
https://doi.org/10.1007/978-1-4757-0241-5

Altin, J. G., & Sloan, E. K. (1997). The role of CD45 and CD45-associated molecules in T cell
activation. *Immunology and Cell Biology*, *75*(5), 430–445.
https://doi.org/10.1038/icb.1997.68

Andison, M. E., & Sivak, J. G. (1994). The functional morphology of the retractor lentis muscle
of a teleost fish, *Astronotus ocellatus*. *Canadian Journal of Zoology*, *72*(11), 1880–1886.
https://doi.org/10.1139/z94-256

Angileri, K. M., & Gross, J. M. (2020). Dnmt1 function is required to maintain retinal stem cells
within the ciliary marginal zone of the zebrafish eye. *Scientific Reports*, *10*(1), 11293.
https://doi.org/10.1038/s41598-020-68016-z

Arredondo, J. L., Fernandes, J. R., & Rao, C. (2008). Ocular Findings in Pediatric Deaths Under
2Years of Age (19942004). *Journal of Forensic Sciences*, *53*(4), 928–934.
https://doi.org/10.1111/j.1556-4029.2008.00757.x

Benfey, T. J., & Methven, D. A. (1986). Pilot-scale rearing of larval and juvenile lumpfish
(Cyclopterus lumpus L.), with some notes on early development. *Aquaculture*, *56*(3–4),
301–306. https://doi.org/10.1016/0044-8486(86)90344-3

Brown, J. A. (1986). The development of feeding behaviour in the lumpfish, Cyclopterus

 lumpus. *Journal of Fish Biology*, *29*(sa), 171–178. https://doi.org/10.1111/j.1095-

 8649.1986.tb05008.x

Brown, J. A., Somerton, D. C., Methven, D. A., & Watkins, J. R. (1992). Recent Advances in

 Lumpfish Cyclopterus lumpus and Ocean Pout Macrozoarces americanus Larviculture.

 Journal of the World Aquaculture Society, *23*(4), 271–276.

 https://doi.org/10.1111/j.1749-7345.1992.tb00790.x

Budke, H., Orazi, A., Neiman, R. S., Cattoretti, G., John, K., & Barberis, M. (1994). Assessment

 of cell proliferation in paraffin sections of normal bone marrow by the monoclonal

 antibodies Ki-67 and PCNA. *Modern Pathology: An Official Journal of the United States

 and Canadian Academy of Pathology, Inc*, *7*(8), 860–866.

Burnside, B., Evans, M., Fletcher, R. T., & Chader, G. J. (1982). Induction of dark-adaptive

 retinomotor movement (cell elongation) in teleost retinal cones by cyclic adenosine 3',’5-

 monophosphate. *Journal of General Physiology*, *79*(5), 759–774.

 https://doi.org/10.1085/jgp.79.5.759

Burnside, B., Wang, E., Pagh-Roehl, K., & Rey, H. (1993). Retinomotor Movements in Isolated

 Teleost Retinal Cone Inner-Outer Segment Preparations (CIS-COS): Effects of Light,

 Dark and Dopamine. *Experimental Eye Research*, *57*(6), 709–722.

 https://doi.org/10.1006/exer.1993.1179

Chattopadhyay, S., Chaklader, M., & Law, S. (2019). Aberrant Wnt Signaling Pathway in the

 Hematopoietic Stem/Progenitor Compartment in Experimental Leukemic Animal.

 Journal of Cell Communication and Signaling, *13*(1), 39–52.

 https://doi.org/10.1007/s12079-018-0470-6

Chettri, J. K., Raida, M. K., Kania, P. W., & Buchmann, K. (2012). Differential immune

    response of rainbow trout (Oncorhynchus mykiss) at early developmental stages (larvae

    and fry) against the bacterial pathogen Yersinia ruckeri. *Developmental & Comparative*

    Immunology, *36*(2), 463–474. https://doi.org/10.1016/j.dci.2011.08.014

Damsgaard, C., Lauridsen, H., Harter, T. S., Kwan, G. T., Thomsen, J. S., Funder, A. M.,

    Supuran, C. T., Tresguerres, M., Matthews, P. G., & Brauner, C. J. (2020). A novel

    acidification mechanism for greatly enhanced oxygen supply to the fish retina. *ELife*, *9*,

    e58995. https://doi.org/10.7554/eLife.58995

DelMonte, D. W., & Kim, T. (2011). Anatomy and physiology of the cornea. *Journal of*

    Cataract and Refractive Surgery, *37*(3), 588–598.

    https://doi.org/10.1016/j.jcrs.2010.12.037

Ding, L., Vezzani, B., Khan, N., Su, J., Xu, L., Yan, G., Liu, Y., Li, R., Gaur, A., Diao, Z., Hu,

    Y., Yang, Z., Hardy, W. R., James, A. W., Sun, H., & Péault, B. (2020). CD10

    expression identifies a subset of human perivascular progenitor cells with high

    proliferation and calcification potentials. *Stem Cells*, *38*(2), 261–275.

    https://doi.org/10.1002/stem.3112

Eriksen, E., Durif, C. M. F., & Prozorkevich, D. (2014). Lumpfish (Cyclopterus lumpus) in the

    Barents Sea: Development of biomass and abundance indices, and spatial distribution.

    ICES Journal of Marine Science, *71*(9), 2398–2402.

    https://doi.org/10.1093/icesjms/fsu059

Fischer, A. J., Bosse, J. L., & El-Hodiri, H. M. (2013). The ciliary marginal zone (CMZ) in

    development and regeneration of the vertebrate eye. *Experimental Eye Research*, *116*,

    199–204. https://doi.org/10.1016/j.exer.2013.08.018

Fritsch, R., Ullmann, J. F. P., Bitton, P.-P., Collin, S. P., & Michiels, N. K. (2017). Optic-nerve-transmitted eyeshine, a new type of light emission from fish eyes. *Frontiers in Zoology*, *14*(1), 14. https://doi.org/10.1186/s12983-017-0198-9

Garcia de Leaniz, C., Gutierrez Rabadan, C., Barrento, S. I., Stringwell, R., Howes, P. N., Whittaker, B. A., Minett, J. F., Smith, R. G., Pooley, C. L., Overland, B. J., Biddiscombe, L., Lloyd, R., Consuegra, S., Maddocks, J. K., Deacon, P. T. J., Jennings, B. T., Rey Planellas, S., Deakin, A., Moore, A. I., … Pavlidis, M. (2022). Addressing the welfare needs of farmed lumpfish: Knowledge gaps, challenges and solutions. *Reviews in Aquaculture*, *14*(1), 139–155. https://doi.org/10.1111/raq.12589

Gendron, R. L., Good, W. V., Adams, L. C., & Paradis, H. (2001). *Suppressed Expression of Tubedown-1 in Retinal Neovascularization of Proliferative Diabetic Retinopathy*. *42*(12), 8.

Gendron, R. L., Liu, C. Y., Paradis, H., Adams, L. C., & Kao, W. W. (2001). MK/T-1, an immortalized fibroblast cell line derived using cultures of mouse corneal stroma. *Molecular Vision*, *7*, 107–113.

Gendron, R. L., Paradis, H., Ahmad, R., Kao, K., Boyce, D., Good, W. V., Kumar, S., Vasquez, I., Cao, T., Hossain, A., Chakraborty, S., Valderrama, K., & Santander, J. (2020). CD10+ Cells and IgM in Pathogen Response in Lumpfish (Cyclopterus lumpus) Eye Tissues. *Frontiers in Immunology*, *11*, 576897. https://doi.org/10.3389/fimmu.2020.576897

Gendron, R. L., Tsai, F.-Y., Paradis, H., & Arceci, R. J. (1996). Induction of Embryonic Vasculogenesis by bFGF and LIFin Vitroand in Vivo. *Developmental Biology*, *177*(1), 332–346. https://doi.org/10.1006/dbio.1996.0167

Georgiadis, A., Tschernutter, M., Bainbridge, J. W. B., Balaggan, K. S., Mowat, F., West, E. L., Munro, P. M. G., Thrasher, A. J., Matter, K., Balda, M. S., & Ali, R. R. (2010). The Tight Junction Associated Signalling Proteins ZO-1 and ZONAB Regulate Retinal Pigment Epithelium Homeostasis in Mice. *PLoS ONE*, *5*(12), e15730. https://doi.org/10.1371/journal.pone.0015730

Geven, E. J. W., & Klaren, P. H. M. (2017). The teleost head kidney: Integrating thyroid and immune signalling. *Developmental & Comparative Immunology*, *66*, 73–83. https://doi.org/10.1016/j.dci.2016.06.025

Goel, M. (2010). Aqueous Humor Dynamics: A Review~!2010-03-03~!2010-06-17~!2010-09-02~! *The Open Ophthalmology Journal*, *4*(1), 52–59. https://doi.org/10.2174/1874364101004010052

Gonzalez, G., Sasamoto, Y., Ksander, B. R., Frank, M. H., & Frank, N. Y. (2018). Limbal stem cells: Identity, developmental origin, and therapeutic potential. *Wiley Interdisciplinary Reviews. Developmental Biology*, *7*(2). https://doi.org/10.1002/wdev.303

Goulet, D., Green, J. M., & Shears, T. H. (1986). Courtship, spawning, and parental care behavior of the lumpfish, *Cyclopterus lumpus* L., in Newfoundland. *Canadian Journal of Zoology*, *64*(6), 1320–1325. https://doi.org/10.1139/z86-196

Graw, J. (2010). Eye Development. In *Current Topics in Developmental Biology* (Vol. 90, pp. 343–386). Elsevier. https://doi.org/10.1016/S0070-2153(10)90010-0

Gregerson, D. S., & Yang, J. (2003). CD45-Positive Cells of the Retina and Their Responsiveness to In Vivo and In Vitro Treatment with IFN-γ or Anti-CD40. *Investigative Opthalmology & Visual Science*, *44*(7), 3083. https://doi.org/10.1167/iovs.02-1014

Gumbiner, B., Lowenkopf, T., & Apatira, D. (1991). Identification of a 160-kDa polypeptide that binds to the tight junction protein ZO-1. *Proceedings of the National Academy of Sciences*, *88*(8), 3460–3464. https://doi.org/10.1073/pnas.88.8.3460

Gupta, M. P., Herzlich, A. A., Sauer, T., & Chan, C.-C. (2015). Retinal Anatomy and Pathology. In Q. D. Nguyen, E. B. Rodrigues, M. E. Farah, W. F. Mieler, & D. V. Do (Eds.), *Developments in Ophthalmology* (Vol. 55, pp. 7–17). S. Karger AG. https://doi.org/10.1159/000431128

Gururaja Rao, S., Patel, N. J., & Singh, H. (2020). Intracellular Chloride Channels: Novel Biomarkers in Diseases. *Frontiers in Physiology*, *11*, 96. https://doi.org/10.3389/fphys.2020.00096

Hasegawa, T., McLeod, D. S., Bhutto, I. A., Prow, T., Merges, C. A., Grebe, R., & Lutty, G. A. (2007). The embryonic human choriocapillaris develops by hemo-vasculogenesis. *Developmental Dynamics*, *236*(8), 2089–2100. https://doi.org/10.1002/dvdy.21231

Heavner, W., & Pevny, L. (2012). Eye Development and Retinogenesis. *Cold Spring Harbor Perspectives in Biology*, *4*(12), a008391–a008391. https://doi.org/10.1101/cshperspect.a008391

Hitchcock, P. F., & Raymond, P. A. (2004). The Teleost Retina as a Model for Developmental and Regeneration Biology. *Zebrafish*, *1*(3), 257–271. https://doi.org/10.1089/zeb.2004.1.257

Imafuku, K., Kamaguchi, M., Natsuga, K., Nakamura, H., Shimizu, H., & Iwata, H. (2021). Zonula occludens-1 demonstrates a unique appearance in buccal mucosa over several layers. *Cell and Tissue Research*, *384*(3), 691–702. https://doi.org/10.1007/s00441-021-03425-8

Imsland, A. K. D., Danielsen, M., Jonassen, T. M., Hangstad, T. A., & Falk-Petersen, I.-B. (2019). Effect of incubation temperature on eggs and larvae of lumpfish (Cyclopterus lumpus). *Aquaculture*, *498*, 217–222. https://doi.org/10.1016/j.aquaculture.2018.08.061

Ingólfsson, A., & Kristjánsson, B. K. (2002). Diet of Juvenile Lumpsucker Cyclopterus lumpus (Cyclopteridae) in Floating Seaweed: Effects of Ontogeny and Prey Availability. *Copeia*, *2002*(2), 472–476. https://doi.org/10.1643/0045-8511(2002)002[0472:DOJLCL]2.0.CO;2

Jagannathan-Bogdan, M., & Zon, L. (2013). *Hematopoiesis—PubMed*. https://pubmed.ncbi.nlm.nih.gov/23715539/

Jana, S., Jha, B., Patel, C., Jana, D., & Agarwal, A. (2014). CD10-A new prognostic stromal marker in breast carcinoma, its utility, limitations and role in breast cancer pathogenesis. *Indian Journal of Pathology and Microbiology*, *57*(4), 530. https://doi.org/10.4103/0377-4929.142639

Juríková, M., Danihel, Ľ., Polák, Š., & Varga, I. (2016). Ki67, PCNA, and MCM proteins: Markers of proliferation in the diagnosis of breast cancer. *Acta Histochemica*, *118*(5), 544–552. https://doi.org/10.1016/j.acthis.2016.05.002

Kelman, Z. (1997). PCNA: Structure, functions and interactions. *Oncogene*, *14*(6), 629–640. https://doi.org/10.1038/sj.onc.1200886

Kennedy, J., Jónsson, S. Þ., Kasper, J. M., & Ólafsson, H. G. (2015). Movements of female lumpfish (Cyclopterus lumpus) around Iceland. *ICES Journal of Marine Science*, *72*(3), 880–889. https://doi.org/10.1093/icesjms/fsu170

Khorramshahi, O., Schartau, J. M., & Kröger, R. H. H. (2008). A complex system of ligaments and a muscle keep the crystalline lens in place in the eyes of bony fishes (teleosts). *Vision Research*, *48*(13), 1503–1508. https://doi.org/10.1016/j.visres.2008.03.017

Kim, C. (2010). Homeostatic and pathogenic extramedullary hematopoiesis. *Journal of Blood Medicine*, 13. https://doi.org/10.2147/JBM.S7224

Kitambi, S. S., Chandrasekar, G., & Addanki, V. K. (2011). Teleost fish – powerful models for studying development, function and diseases of the human eye. *Current Science*, *100*(12), 1815–1823. JSTOR.

Kobayashi, I., Katakura, F., & Moritomo, T. (2016). Isolation and characterization of hematopoietic stem cells in teleost fish. *Developmental & Comparative Immunology*, *58*, 86–94. https://doi.org/10.1016/j.dci.2016.01.003

Kolb, H. (2007). *Outer Plexiform Layer*. 17.

Kolb, H. (2012). Simple Anatomy of the Retina. In H. Kolb, E. Fernandez, & R. Nelson (Eds.), *Webvision: The Organization of the Retina and Visual System*. University of Utah Health Sciences Center. http://www.ncbi.nlm.nih.gov/books/NBK11533/

Kolosov, D., Bui, P., Chasiotis, H., & Kelly, S. P. (2013). Claudins in teleost fishes. *Tissue Barriers*, *1*(3), e25391. https://doi.org/10.4161/tisb.25391

Kunz, Y. W. (2004). *Developmental Biology of Teleost Fishes*. Springer Netherlands. https://doi.org/10.1007/978-1-4020-2997-4

Laemmli, U. K. (1970). Cleavage of Structural Proteins during the Assembly of the Head of Bacteriophage T4. *Nature*, *227*(5259), 680–685. https://doi.org/10.1038/227680a0

Leung, A. Y., Leung, J. C., Chan, L. Y., Ma, E. S., Kwan, T. T., Lai, K., Meng, A., & Liang, R. (2005). Proliferating cell nuclear antigen (PCNA) as a proliferative marker during embryonic and adult zebrafish hematopoiesis. *Histochemistry and Cell Biology*, *124*(2), 105–111. https://doi.org/10.1007/s00418-005-0003-2

Maguer-Satta, V., Besançon, R., & Bachelard-Cascales, E. (2011). Concise Review: Neutral

    Endopeptidase (CD10): A Multifaceted Environment Actor in Stem Cells, Physiological

    Mechanisms, and Cancer. *Stem Cells*, *29*(3), 389–396. https://doi.org/10.1002/stem.592

Marozzi, C., Bertoni, F., Randelli, E., Buonocore, F., Timperio, A. M., & Scapigliati, G. (2012).

    A monoclonal antibody for the CD45 receptor in the teleost fish Dicentrarchus labrax.

    Developmental & Comparative Immunology, *37*(3–4), 342–353.

    https://doi.org/10.1016/j.dci.2012.03.015

Masri, R. A., Weltzien, F., Purushothuman, S., Lee, S. C. S., Martin, P. R., & Grünert, U. (2021).

    Composition of the Inner Nuclear Layer in Human Retina. *Investigative Opthalmology &*

    Visual Science, *62*(9), 22. https://doi.org/10.1167/iovs.62.9.22

Momen, A. I., Muir, R. T., Barnett, C., & Sundaram, A. N. E. (2020). Homonymous Retinal

    Ganglion Cell Layer Atrophy With Asymptomatic Optic Tract Glioma in

    Neurofibromatosis Type I. *Frontiers in Neurology*, *11*, 256.

    https://doi.org/10.3389/fneur.2020.00256

Moneghini, L., Tosi, D., Graziani, D., Caretti, A., Colletti, G., Baraldini, V., Cattaneo, E.,

    Spaccini, L., Zocca, A., & Bulfamante, G. P. (2020). CD10 and CD34 as markers in

    vascular malformations with PIK3CA and TEK mutations. *Human Pathology*, *99*, 98–

    106. https://doi.org/10.1016/j.humpath.2020.04.001

Mortensen, A., Johansen, R. B., Hansen, Ø. J., & Puvanendran, V. (2020). Temperature

    preference of juvenile lumpfish (Cyclopterus lumpus) originating from the southern and

    northern parts of Norway. *Journal of Thermal Biology*, *89*, 102562.

    https://doi.org/10.1016/j.jtherbio.2020.102562

Murthy, K. R., Goel, R., Subbannayya, Y., Jacob, H. K., Murthy, P. R., Manda, S. S., Patil, A. H., Sharma, R., Sahasrabuddhe, N. A., Parashar, A., Nair, B. G., Krishna, V., Prasad, T. K., Gowda, H., & Pandey, A. (2014). Proteomic analysis of human vitreous humor. *Clinical Proteomics*, *11*(1), 29. https://doi.org/10.1186/1559-0275-11-29

Nickla, D. L., & Wallman, J. (2010). The multifunctional choroid. *Progress in Retinal and Eye Research*, *29*(2), 144–168. https://doi.org/10.1016/j.preteyeres.2009.12.002

Ollivier, F. J., Samuelson, D. A., Brooks, D. E., Lewis, P. A., Kallberg, M. E., & Komaromy, A. M. (2004). Comparative morphology of the tapetum lucidum (among selected species). *Veterinary Ophthalmology*, *7*(1), 11–22. https://doi.org/10.1111/j.1463-5224.2004.00318.x

Otteson, D. C., & Hitchcock, P. F. (2003). Stem cells in the teleost retina: Persistent neurogenesis and injury-induced regeneration. *Vision Research*, *43*(8), 927–936. https://doi.org/10.1016/S0042-6989(02)00400-5

Ozaki, S., Umakoshi, A., Yano, H., Ohsumi, S., Sumida, Y., Hayase, E., Usa, E., Islam, A., Choudhury, M. E., Nishi, Y., Yamashita, D., Ohtsuka, Y., Nishikawa, M., Inoue, A., Suehiro, S., Kuwabara, J., Watanabe, H., Takada, Y., Watanabe, Y., … Tanaka, J. (2021). Chloride intracellular channel protein 2 is secreted and inhibits MMP14 activity, while preventing tumor cell invasion and metastasis. *Neoplasia*, *23*(8), 754–765. https://doi.org/10.1016/j.neo.2021.06.001

Paradis, H., Islam, T., Tucker, S., Tao, L., Koubi, S., & Gendron, R. L. (2008). Tubedown associates with cortactin and controls permeability of retinal endothelial cells to albumin. *Journal of Cell Science*, *121*(12), 1965–1972. https://doi.org/10.1242/jcs.028597

Powell, A., Treasurer, J. W., Pooley, C. L., Keay, A. J., Lloyd, R., Imsland, A. K., & Garcia de

   Leaniz, C. (2018). Use of lumpfish for sea-lice control in salmon farming: Challenges

   and opportunities. *Reviews in Aquaculture*, *10*(3), 683–702.

   https://doi.org/10.1111/raq.12194

Press, C. McL., & Evensen, Ø. (1999). The morphology of the immune system in teleost fishes.

   Fish & Shellfish Immunology, *9*(4), 309–318. https://doi.org/10.1006/fsim.1998.0181

Reh, T. A., & Fischer, A. J. (2001). Stem Cells in the Vertebrate Retina. *Brain, Behavior and

   Evolution*, *58*(5), 296–305. https://doi.org/10.1159/000057571

Rheinländer, A., Schraven, B., & Bommhardt, U. (2018). CD45 in human physiology and

   clinical medicine. *Immunology Letters*, *196*, 22–32.

   https://doi.org/10.1016/j.imlet.2018.01.009

Ruan, X., Liu, Z., Luo, L., & Liu, Y. (2020). The Structure of the Lens and Its Associations with

   the Visual Quality. *BMJ Open Ophthalmology*, *5*(1), e000459.

   https://doi.org/10.1136/bmjophth-2020-000459

Shaham, O., Menuchin, Y., Farhy, C., & Ashery-Padan, R. (2012). Pax6: A multi-level regulator

   of ocular development. *Progress in Retinal and Eye Research*, *31*(5), 351–376.

   https://doi.org/10.1016/j.preteyeres.2012.04.002

Sherpa, T., Fimbel, S. M., Mallory, D. E., Maaswinkel, H., Spritzer, S. D., Sand, J. A., Li, L.,

   Hyde, D. R., & Stenkamp, D. L. (2008). Ganglion cell regeneration following whole-

   retina destruction in zebrafish. *Developmental Neurobiology*, *68*(2), 166–181.

   https://doi.org/10.1002/dneu.20568

Somiya, H. (1980). Fishes with Eye Shine: Functional Morphology of Guanine Type Tapetum

   Lucidum. *Marine Ecology Progress Series*, *2*, 9–26. https://doi.org/10.3354/meps002009

Somiya, H. (1987). Dynamic mechanism of visual accommodation in teleosts: Structure of the

    lens muscle and its nerve control. *Proceedings of the Royal Society of London. Series B.*

    Biological Sciences, *230*(1258), 77–91. https://doi.org/10.1098/rspb.1987.0010

Soules, K. A., & Link, B. A. (2005). Morphogenesis of the anterior segment in the zebrafish eye.

    BMC Developmental Biology, *5*(1), 12. https://doi.org/10.1186/1471-213X-5-12

Stevenson, B. R., Siliciano, J. D., Mooseker, M. S., & Goodenough, D. A. (1986). Identification

    of ZO-1: A high molecular weight polypeptide associated with the tight junction (zonula

    occludens) in a variety of epithelia. *The Journal of Cell Biology*, *103*(3), 755–766.

    https://doi.org/10.1083/jcb.103.3.755

Strauss, O. (2005). The Retinal Pigment Epithelium in Visual Function. *Physiological Reviews*,

    85(3), 845–881. https://doi.org/10.1152/physrev.00021.2004

Tornavaca, O., Chia, M., Dufton, N., Almagro, L. O., Conway, D. E., Randi, A. M., Schwartz,

    M. A., Matter, K., & Balda, M. S. (2015). ZO-1 controls endothelial adherens junctions,

    cell–cell tension, angiogenesis, and barrier formation. *Journal of Cell Biology*, *208*(6),

    821–838. https://doi.org/10.1083/jcb.201404140

Tsin, A., Betts-Obregon, B., & Grigsby, J. (2018). Visual cycle proteins: Structure, function, and

    roles in human retinal disease. *Journal of Biological Chemistry*, *293*(34), 13016–13021.

    https://doi.org/10.1074/jbc.AW118.003228

Ubels, L., Edelhauser, P., & Antoike, E. (1984). *Choroidal R&e Mircrbile Function and*

    Resistance to Retinal Oxygen Toxicity in Fish. 10.

Ueno, Y., Ozaki, S., Umakoshi, A., Yano, H., Choudhury, M. E., Abe, N., Sumida, Y.,

    Kuwabara, J., Uchida, R., Islam, A., Ogawa, K., Ishimaru, K., Yorozuya, T., Kunieda, T.,

    Watanabe, Y., Takada, Y., & Tanaka, J. (2019). Chloride intracellular channel protein 2

in cancer and non-cancer human tissues: Relationship with tight junctions. *Tissue Barriers*, *7*(1), 1593775. https://doi.org/10.1080/21688370.2019.1593775

Umeda, K., Ikenouchi, J., Katahira-Tayama, S., Furuse, K., Sasaki, H., Nakayama, M., Matsui, T., Tsukita, S., Furuse, M., & Tsukita, S. (2006). ZO-1 and ZO-2 Independently Determine Where Claudins Are Polymerized in Tight-Junction Strand Formation. *Cell*, *126*(4), 741–754. https://doi.org/10.1016/j.cell.2006.06.043

Van Buskirk, E. M. (1989). The anatomy of the limbus. *Eye*, *3*(2), 101–108. https://doi.org/10.1038/eye.1989.16

Van den Bogerd, B., Zakaria, N., Adam, B., Matthyssen, S., Koppen, C., & Ní Dhubhghaill, S. (2019). Corneal Endothelial Cells Over the Past Decade: Are We Missing the Mark(er)? *Translational Vision Science & Technology*, *8*(6), 13. https://doi.org/10.1167/tvst.8.6.13

Wang, S.-C. (2014). PCNA: A silent housekeeper or a potential therapeutic target? *Trends in Pharmacological Sciences*, *35*(4), 178–186. https://doi.org/10.1016/j.tips.2014.02.004

Willoughby, C. E., Ponzin, D., Ferrari, S., Lobo, A., Landau, K., & Omidi, Y. (2010). Anatomy and physiology of the human eye: Effects of mucopolysaccharidoses disease on structure and function - a review: Anatomy and physiology of the eye. *Clinical & Experimental Ophthalmology*, *38*, 2–11. https://doi.org/10.1111/j.1442-9071.2010.02363.x

Witten, P. E., Harris, M. P., Huysseune, A., & Winkler, C. (2017). Small teleost fish provide new insights into human skeletal diseases. In *Methods in Cell Biology* (Vol. 138, pp. 321–346). Elsevier. https://doi.org/10.1016/bs.mcb.2016.09.001

Wittenberg, J. B., & Haedrich, R. L. (1974). THE CHOROID RETE MIRABILE OF THE FISH EYE. II. DISTRIBUTION AND RELATION TO THE PSEUDOBRANCH AND TO

THE SWIMBLADDER RETE MIRABILE. *The Biological Bulletin*, *146*(1), 137–156.

    https://doi.org/10.2307/1540403

Wittenberg, J. B., & Wittenberg, B. A. (1974). THE CHOROID RETE MIRABILE OF THE

    FISH EYE. I. OXYGEN SECRETION AND STRUCTURE: COMPARISON WITH

    THE SWIMBLADDER RETE MIRABILE. *The Biological Bulletin*, *146*(1), 116–136.

    https://doi.org/10.2307/1540402

Yamamoto, K., Miwa, Y., Abe-Suzuki, S., Abe, S., Kirimura, S., Onishi, I., Kitagawa, M., &

    Kurata, M. (2016). Extramedullary hematopoiesis: Elucidating the function of the

    hematopoietic stem cell niche (Review). *Molecular Medicine Reports*, *13*(1), 587–591.

    https://doi.org/10.3892/mmr.2015.4621

Zachary, J. F. (2017). *Pathologic basis of veterinary disease* (Sixth edition). Elsevier.

Zeng, J., Li, Z., Lui, E. Y., Lam, S. H., & Swaminathan, K. (2018). Tilapia and human CLIC2

    structures are highly conserved. *Biochemical and Biophysical Research Communications*,

    495(2), 1752–1757. https://doi.org/10.1016/j.bbrc.2017.11.189

Zhang, T., Kho, A. M., & Srinivasan, V. J. (2021). In vivo Morphometry of Inner Plexiform

    Layer (IPL) Stratification in the Human Retina With Visible Light Optical Coherence

    Tomography. *Frontiers in Cellular Neuroscience*, *15*, 655096.

    https://doi.org/10.3389/fncel.2021.655096

Appendix 1: Animal Care Approval 2-(17-03-RG) Lumpfish as model for studying vision health and fitness of ocean Teleostei

Animal Care Committee (ACC)
St. John's, NL, Canada A1C 5S7
Tel: 709 777-6620 acs@mun.ca

https://www.mun.ca/research/about/acs/acc/

Dear: Dr. Robert Gendron, Faculty of Medicine\Division of BioMedical Sciences

Researcher Portal File No.: 20210789
Animal Care File: 17-03-RG
Entitled: 2-(17-03-RG) Lumpfish as a model for studying vision health and fitness of ocean Teleostei
Related Awards:

Awards File No	Title		Status
2018 0034	Lumpfish (Teleostei) as a model for studying dietary vitamin A in vision health and fitness	Completed	1. Research Grant and Contract Services (RGCS) – St. John's and Grenfell Campuses
2019 2237	Mechanisms of cell growth and development	Active	1. Research Grant and Contract Services (RGCS) – St. John's and Grenfell Campuses
2020 1808	Investigation of ocular extramedullary hematopoiesis during development	Active	1. Research Grant and Contract Services (RGCS) – St. John's and Grenfell Campuses

2021 1293	Impact of vitamin A dietary supplementation on lumpfish visual health and cataract development	Active	1. Research Grant and Contract Services (RGCS) – St. John's and Grenfell Campuses
2021 1294	Molecular and cellular biology of the lumpfish eye	Active	1. Research Grant and Contract Services (RGCS) – St. John's and Grenfell Campuses

Approval Date: September 01, 2020
Next Annual Report Due: September 01, 2022
Ethics Clearance Expires: September 01, 2023

███████████████████████████████████

Your Annual Report was reviewed by the IACC and approved.

Animal use records will be compiled and reported to the Canadian Council on Animal Care.

NOTE: You can access a copy of this email at any time under the "Shared Communications" section of the Logs tab of your file in the Memorial Researcher Portal.
Sincerely,

MARIE WASEF I ACC COORDINATOR
Department of Animal Care Services
Memorial University of Newfoundland
Health Sciences Centre I Room H1848
P: 709-777-6621
E-Mail: maw222@mun.ca

 <grammarly-desktop-integration data-grammarly-shadow-root="true"></grammarly-desktop-integration>